DOI: 10.1002/cmdc.200800414

Tacrine–Melatonin Hybrids as Multifunctional Agents for Alzheimer's Disease, with Cholinergic, Antioxidant, and Neuroprotective Properties

María Isabel Fernández-Bachiller,[a] Concepción Pérez,[a] Nuria Eugenia Campillo,[a] Juan Antonio Páez,[a] Gema Cristina González-Muñoz,[a] Paola Usán,[b] Esther García-Palomero,[b] Manuela G. López,[c] Mercedes Villarroya,[c] Antonio G. García,[c, d] Ana Martínez,[b, e] and María Isabel Rodríguez-Franco*[a]

Tacrine–melatonin hybrids were designed and synthesized as new multifunctional drug candidates for Alzheimer's disease. These compounds may simultaneously palliate intellectual deficits and protect the brain against both β-amyloid (Aβ) peptide and oxidative stress. They show improved cholinergic and antioxidant properties, and are more potent and selective inhibitors of human acetylcholinesterase (hAChE) than tacrine. They also capture free radicals better than melatonin. Molecular modeling studies show that these hybrids target both the catalytic active site (CAS) and the peripheral anionic site (PAS) of AChE. At sub-micromolar concentrations they efficiently displace the binding of propidium iodide from the PAS and could thus inhibit Aβ peptide aggregation promoted by AChE. Moreover, they also inhibit Aβ self-aggregation and display neuroprotective properties in a human neuroblastoma line against cell death induced by various toxic insults, such as $A\beta_{25-35}$, H_2O_2, and rotenone. Finally, they exhibit low toxicity and may be able to penetrate the central nervous system according to an in vitro parallel artificial membrane permeability assay for the blood–brain barrier (PAMPA-BBB).

Introduction

Alzheimer's disease (AD), the most common cause of dementia in elderly people, is a complex neurodegenerative illness of the central nervous system (CNS), characterized by progressive memory loss and other cognitive impairments. The etiology of AD is not completely known, although there are diverse hallmarks such as β-amyloid (Aβ) deposits, τ-protein aggregation, oxidative damage in cell structures, and low levels of acetylcholine (ACh) that seem to play significant roles in the disease.[1]

Several pharmacological strategies have emerged over the last decades including cholinergic[2] and noncholinergic interventions.[3] The cholinergic approach launched four drugs on the market for management of the disease: the acetylcholinesterase inhibitors (AChE-Is) tacrine, donepezil, rivastigmine, and galantamine, which increase neurotransmission at cholinergic synapses in the brain, improving cognition.[4] The only approved noncholinergic drug for AD is memantine, an *N*-methyl-D-aspartate (NMDA) receptor antagonist, which improves cognition and mental functions by restoration of homeostasis in the glutamatergic system.[5] Nowadays many candidates with other pharmacological profiles are in phase III clinical trials, such as the γ-secretase inhibitor LY450139, the presenilin modulator docosahexaenoic acid, the PPAR-γ agonist rosiglitazone, and the anticholesterol agent simvastatin, among others.[6]

To date, the approved AChE-Is have been considered as simple symptomatic short-term drugs that improve memory but do not stop neurodegeneration. However, clinical data emerging from long-term trials suggests that the rate of neurodegenerative progression of AD is decreased in patients treated with these drugs, and that a disease-modifying effect may take place.[7] Moreover, the recent development of neuroimaging techniques has provided empirical evidence of these beneficial effects, showing that patients treated with AChE-Is do not show the widespread cortical atrophic changes associated with AD.[8]

The disease-modifying effects observed with the use of AChE-Is might be related to their primary mode of action or

[a] *Dr. M. I. Fernández-Bachiller, Dr. C. Pérez, Dr. N. E. Campillo, Dr. J. A. Páez, G. C. González-Muñoz, Dr. M. I. Rodríguez-Franco*
Instituto de Química Médica
Consejo Superior de Investigaciones Científicas (CSIC)
C/Juan de la Cierva 3, 28006 Madrid (Spain)
Fax: (+34) 915 644 853
E-mail: IsabelRguez@iqm.csic.es

[b] *P. Usán, Dr. E. García-Palomero, Dr. A. Martínez*
Noscira S.A., Avda. de la Industria 52, 28760 Madrid (Spain)

[c] *Dr. M. G. López, Dr. M. Villarroya, Dr. A. G. García*
Instituto Teófilo Hernando, Facultad de Medicina
Universidad Autónoma de Madrid (UAM)
C/Arzobispo Morcillo 4, 28029 Madrid (Spain)

[d] *Dr. A. G. García*
Servicio de Farmacología Clínica
Hospital Universitario de la Princesa
C/Diego de León 62, 28006 Madrid (Spain)

[e] *Dr. A. Martínez*
current address: Instituto de Química Médica (CSIC)
C/Juan de la Cierva 3, 28006 Madrid (Spain)

their binding with other neuronal targets (NMDA, nicotinic, or muscarinic receptors)[9] or even their interaction with the amyloid cascade.[10] Biochemical studies have indicated that AChE directly induces the assembly of Aβ peptides into amyloid fibrils, forming stable AChE–Aβ complexes, which are more toxic than Aβ peptides alone.[11] Because the adhesion function of AChE to Aβ is located at the peripheral anionic site (PAS),[12] inhibitors that are able to bind both the catalytic active site (CAS) and PAS are of particular interest in AD, as they can simultaneously improve memory and slow the rate of amyloid degeneration.[13] For this reason, the interest in these dual-site inhibitors has increased in recent years, with NP-61 being the first compound of this class in phase I clinical trials for Alzheimer's disease.[14]

During aging, the endogenous antioxidant defense system progressively decays, and an increasing body of evidence supports the early involvement of oxidative stress in the pathogenesis and progression of AD.[15] Recent research has demonstrated that oxidative damage is an event that precedes the appearance of other pathological hallmarks of the disease, namely senile plaques and neurofibrillary tangles.[16] Thus, drugs that specifically scavenge oxygen radicals could be useful for either the prevention or treatment of AD.[17]

Tacrine (**1**), the first drug approved for AD, is a potent nonselective inhibitor of both AChE and butyrylcholinesterase (BuChE). Although hepatotoxicity has limited the therapeutic use of this drug, the search for tacrine analogues is still of interest in AD research.[18] Melatonin (**2**) is a pineal neurohormone, the levels of which decrease during aging, especially in AD patients. It has been reported to possess strong antioxidant activity, and is able to directly scavenge a variety of reactive oxygen species (ROS).[19] Melatonin also stimulates several endogenous antioxidative enzymes, improves mitochondrial energy metabolism, decreases neurofilament hyperphosphorylation, and plays a neuroprotective role against Aβ.[20]

Continuing with our research on various heterocyclic compound families with potential application in AD,[21] and taking into account that drugs with two or more useful biological activities for the same pathology may represent an important pharmacological advance,[22] we are currently interested in multifunctional drugs that combine potent dual binding to both the CAS and PAS of AChE and neuroprotective properties in a single small molecule. Tacrine–melatonin hybrids (**3**–**25**) were designed by using moieties with well-known properties for each biological activity: **1** for the inhibition of AChE through its binding to the CAS, and **2** for both its neuroprotective properties and its interaction with the PAS. Regarding the CAS of AChE, which is located at the bottom of a deep gorge, we considered tethering these two fragments with hydrocarbon chains, following a previously described strategy.[23] These flexible linkers could be accommodated by the enzyme cavity, allowing simultaneous interaction with the CAS and PAS of AChE (Figure 1).

In this field, we reported preliminary results on the synthesis and biological evaluation of tacrine–melatonin hybrids that show better AChE inhibitory and antioxidant properties than their separate structures.[24] Prompted by their promising biological profile, we describe herein the synthesis of new tacrine–melatonin hybrids in order to have a broader chemical structure–biological activity relationship analysis by molecular modeling, and to study additional pharmacological properties such as propidium iodide displacement from AChE, effects on Aβ self-aggregation, and cell viability. We also studied the neuroprotective effects of these hybrids against death induced in neuroblastoma cells by various toxic insults related to Aβ degeneration ($A\beta_{25-35}$), as well as oxidative stress triggered by hydrogen peroxide and rotenone.

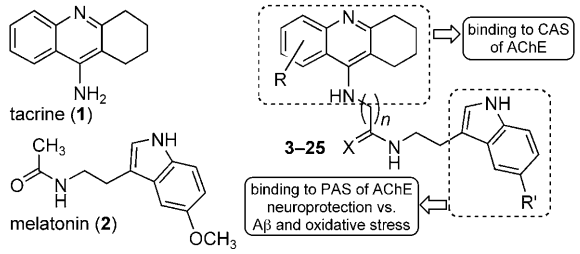

Figure 1. Design strategy for tacrine–melatonin hybrids **3**–**25** (see Table 1 for definitions of R, R′, X, and *n*).

Results and Discussion

Synthesis

Scheme 1 depicts the general procedure for the synthesis of tacrine–melatonin hybrids **3**–**25**. The treatment of 9-chloro-1,2,3,4-tetrahydroacridines **26**–**30**, obtained by published methods,[25] with various α,ω-amino acids in *n*-pentanol at reflux overnight, and subsequent hydrolysis of the pentyl ester intermediates with sodium hydroxide in a mixture of dioxane/H_2O (1:1) at reflux yielded acids **31**–**35** in good yields. These acids were suitably activated with (benzotriazol-1-yloxy)tris(dimethylamino)phosphonium hexafluorophosphate (BOP) and subsequently coupled with commercially available amines

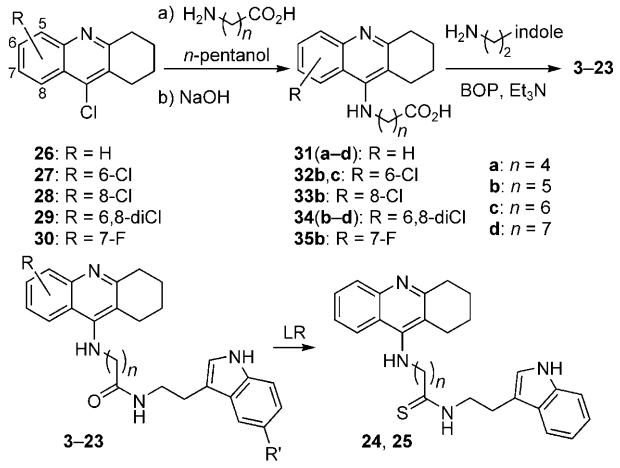

Scheme 1. Synthesis of tacrine–melatonin derivatives.

Table 1. Inhibition of cholinesterases by tacrine–melatonin hybrids, tacrine, and melatonin, along with oxygen radical absorbance capacity (ORAC).[a]

Compd[b]	R	*n*	X	R′	IC_{50} [nM] AChE[c]	BuChE[d]	hAChE[e]	hBuChE[e]	Selectivity for hAChE[f]	Trolox [equiv][g]
3	H	4	O	H	20.0 ± 0.8	12 ± 1	3.0 ± 0.1	5.0 ± 0.2	2	ND
4	H	5	O	H	4.0 ± 0.2	12 ± 1	0.35 ± 0.01	2.5 ± 0.1	7	3.6 ± 0.1
5	H	6	O	H	1.0 ± 0.1	0.95 ± 0.05	0.5 ± 0.02	6.8 ± 0.3	14	3.3 ± 0.1
6	H	7	O	H	2.5 ± 0.1	2.5 ± 0.1	0.8 ± 0.05	5.0 ± 0.2	6	ND
7	6-Cl	5	O	H	2.0 ± 0.1	5.2 ± 0.3	0.725 ± 0.03	175 ± 5	241	2.2 ± 0.1
8	6-Cl	6	O	H	0.2 ± 0.01	8.1 ± 0.3	0.1 ± 0.05	35 ± 2	350	2.1 ± 0.03
9	8-Cl	5	O	H	65 ± 3	15 ± 1	0.87 ± 0.04	23 ± 2	26	4.0 ± 0.1
10	6,8-diCl	5	O	H	3.5 ± 0.2	8.2 ± 0.3	0.7 ± 0.03	250 ± 8	357	1.9 ± 0.1
11	6,8-diCl	6	O	H	2.0 ± 0.1	85 ± 4	0.008 ± 0.0004	7.8 ± 0.4	975	2.5 ± 0.1
12	6,8-diCl	7	O	H	15 ± 0.6	10 ± 0.5	ND	ND	–	ND
13	7-F	5	O	H	36 ± 2	30 ± 1	ND	ND	–	ND
14	H	4	O	OCH_3	35 ± 1	1.8 ± 0.1	2.5 ± 0.4	2.5 ± 0.3	1	ND
15	H	5	O	OCH_3	9.0 ± 0.3	2.0 ± 0.1	0.8 ± 0.04	1.5 ± 0.01	2	1.5 ± 0.1
16	H	6	O	OCH_3	2.3 ± 0.1	2.5 ± 0.1	0.65 ± 0.03	3.0 ± 0.2	5	2.7 ± 0.1
17	H	7	O	OCH_3	20 ± 1	3.0 ± 0.1	5.0 ± 0.4	2.5 ± 0.1	–	ND
18	6-Cl	5	O	OCH_3	12 ± 1	55 ± 2	3.0 ± 0.4	150 ± 5	50	ND
19	8-Cl	5	O	OCH_3	25 ± 1	22 ± 1	0.65 ± 0.05	15 ± 1	23	1.9 ± 0.1
20	6,8-diCl	5	O	OCH_3	4.0 ± 0.2	50 ± 1	ND	ND	–	ND
21	6,8-diCl	6	O	OCH_3	5.0 ± 0.3	100 ± 4	0.04 ± 0.002	25 ± 1	625	1.7 ± 0.01
22	H	5	O	OH	35 ± 2	3.5 ± 0.2	0.45 ± 0.02	1.0 ± 0.1	2	3.2 ± 0.2
23	H	7	O	OH	25 ± 1	2.5 ± 0.1	ND	ND	–	ND
24	H	5	S	H	6.5 ± 0.2	15 ± 0.5	ND	ND	–	ND
25	H	7	S	H	40 ± 1	10 ± 0.5	ND	ND	–	ND
1					40 ± 2	10 ± 0.4	350 ± 10	40 ± 2	–	< 0.01
2					> 100	> 100	ND	ND	–	2.3 ± 0.1

[a] Results are presented as the mean ± SD ($n = 3$); ND: not determined. [b] See Scheme 1 for chemical structures. [c] AChE from bovine erythrocytes. [d] BuChE from horse serum. [e] Enzymes from human source. [f] Selectivity for hAChE = [IC_{50} (hBuChE)]/[IC_{50} (hAChE)]. [g] Data are expressed as (μmol trolox)/(μmol tested compound).

(tryptamine, 5-methoxytryptamine, and serotonin) in the presence of triethylamine in dichloromethane solutions at room temperature to afford the desired tacrine–melatonin amides **3**–**23**. Bioisosteric transformation of the amide into the thioamide group was carried out by using Lawesson's reagent (LR). Thus, the treatment of **4** and **6** with 1.5 equivalents of LR in toluene at reflux afforded the thioamide hybrids **24** and **25** in good yields.

All tacrine–melatonin hybrids were purified by chromatographic techniques and then transformed into their hydrochloride salts by treatment with gaseous hydrochloric acid in dichloromethane solution. Free bases were used to obtain spectroscopic (^{1}H NMR, ^{13}C NMR, IR, and MS) data, and hydrochloride salts were employed to determine both purity (HPLC and combustion analysis) and biological activities (cholinergic, antioxidant, CNS penetration, and neuroprotective properties).

Cholinergic and antioxidant activities

The tacrine–melatonin hybrids were tested as inhibitors of AChE and BuChE by following the method of Ellman et al.[26] Initially, these compounds were evaluated against mammalian enzymes, specifically AChE from bovine erythrocytes and BuChE from horse serum. These enzymes were chosen owing to their lower cost and their high degree of sequence identity to the human enzymes.[27] Tacrine (**1**) and melatonin (**2**) were also tested for comparative purposes (Table 1). All tacrine–melatonin derivatives were found to be potent inhibitors of mammalian cholinesterases at the low-nanomolar concentration range, better than tacrine. As expected, melatonin did not inhibit either enzyme.

Comparing hybrids with the same substituent in each heterocycle, compounds with a 5- or 6-methylene linker between the amine and the amide groups showed better inhibition of AChE than molecules with a 4- or a 7-methylene chain. The introduction of a chlorine atom at position 8 or a fluorine atom at position 7 of the tacrine framework decreased the inhibitory activity toward both enzymes (compounds **9**, **13**, and **19**). However, compounds derived from 6-chlorotacrine (**7** and **8**) and 6,8-dichlorotacrine (**10** and **11**) were more potent and selective AChE inhibitors than their unsubstituted counterparts (**4** and **5**). Finally, replacement of the amide by a thioamide group afforded compounds **24** and **25**, which are less potent than their respective counterparts **4** and **6**.

Then the tacrine–melatonin hybrids were evaluated as inhibitors of human cholinesterases and as free radical scavengers (Table 1). All hybrids potently inhibited human AChE (hAChE), with IC_{50} values in the nanomolar and picomolar ranges (5×10^{-9}–8×10^{-12} M), reflecting 70- to 43 000-fold greater potency than tacrine.

In general, the relationships between chemical structure and the inhibition of human cholinesterases are similar to those found with enzymes from other mammalian sources. From the IC_{50} values of compounds **4**, **5**, and **7**–**11** bearing an unsubstituted indole, it appears that variations on the tacrine fragment influence both potency and selectivity toward hAChE. The

presence of a chlorine atom at position 6 improved both factors; hybrid **8** is a low sub-nanomolar hAChE inhibitor with good selectivity for this enzyme. The potency toward hAChE decreased in the case of compound **9**, in which the chlorine is at position 8 of the tacrine framework, revealing that this change in the structure is not well tolerated by the enzyme. Finally, disubstituted 6,8-dichlorotacrine derivative **11** is the most potent and selective hAChE inhibitor of this series, indicating that the two chlorine atoms could act synergistically in the active site. This compound exhibited an IC_{50} value of 0.008 nM toward hAChE, which is 43000-fold more potent than tacrine, and showed remarkable selectivity: ~1000-fold more active toward hAChE than hBuChE. Finally, regarding modifications to the indole fragment, the introduction of a methoxy or hydroxy group at position 5 gave rise to compounds with inferior values for both potency and selectivity toward hAChE.

Table 2. Permeability results from the PAMPA-BBB assay for 20 commercial drugs (used in experimental validation) and tacrine–melatonin hybrids with their predictive penetration in the CNS.

Compd	P_{epubd} [10^{-6} cm s^{-1}][a]	P_{eexptl} [10^{-6} cm s^{-1}][b]	Compd	P_{eexptl} [10^{-6} cm s^{-1}][b]	Prediction
testosterone	17.0	13.0 ± 0.4	**3**	12.1 ± 0.5	CNS+
verapamil	16.0	13.0 ± 0.5	**4**	11.0 ± 0.5	CNS+
imipramine	13.0	9.1 ± 0.4	**5**	9.2 ± 0.4	CNS+
desipramine	12.0	11.0 ± 0.5	**6**	8.7 ± 0.4	CNS+
astemizole	11.0	11.0 ± 0.4	**7**	7.7 ± 0.3	CNS+
progesterone	9.3	8.6 ± 0.4	**8**	6.9 ± 0.3	CNS+
promazine	8.8	7.3 ± 0.3	**9**	5.2 ± 0.1	CNS+
chlorpromazine	6.5	6.1 ± 0.2	**10**	8.4 ± 0.2	CNS+
clonidine	5.3	6.8 ± 0.2	**11**	7.6 ± 0.3	CNS+
corticosterone	5.1	7.2 ± 0.3	**12**	6.1 ± 0.2	CNS+
piroxicam	2.5	2.3 ± 0.1	**13**	6.4 ± 0.3	CNS+
hydrocortisone	1.9	3.2 ± 0.1	**14**	9.3 ± 0.2	CNS+
aldosterone	1.2	2.7 ± 0.1	**15**	7.7 ± 0.1	CNS+
lomefloxacin	1.1	1.3 ± 0.05	**16**	8.6 ± 0.3	CNS+
enoxacin	0.9	1.7 ± 0.06	**17**	7.9 ± 0.2	CNS+
atenolol	0.8	2.0 ± 0.1	**18**	8.0 ± 0.2	CNS+
ofloxacin	0.8	1.8 ± 0.07	**19**	8.9 ± 0.1	CNS+
isoxicam	0.3	1.6 ± 0.07	**20**	9.6 ± 0.4	CNS+
theophylline	0.1	1.5 ± 0.05	**21**	8.8 ± 0.4	CNS+
cimetidine	0.0	1.2 ± 0.05	**22**	2.0 ± 0.1	CNS−
			23	2.8 ± 0.2	CNS−
			25	6.8 ± 0.3	CNS+

[a] Published values from reference [31]. [b] Data are the mean ± SD of three independent experiments.

Owing to their potency and selectivity toward hAChE, these tacrine–melatonin hybrids should mostly activate central cholinergic transmission, improving mental abilities, and be free of the peripheral side effects related to nonselective cholinesterase inhibitors like tacrine.[28]

The antioxidant activities of tacrine–melatonin hybrids were determined by their competition with fluorescein in the capture of oxygen radicals, thermally generated from 2,2′-azobis-(amidinopropane) dihydrochloride, following a well-established method (ORAC-FL).[29] Trolox, a vitamin E analogue, was used as standard, and the results were expressed as trolox equivalents [(μmol trolox)/(μmol tested compound)] (Table 1). Tacrine showed negligible radical-capture capacity, whereas melatonin had an ORAC-FL value 2.3-fold higher than that of trolox. This activity fully agrees with the value previously described for melatonin (ORAC = 2.0),[30] pointing out the reliability of our experiments. Tested compounds showed potent peroxyl radical absorbance capacities ranging from 1.5- to 4-fold the trolox value. Regarding the indole structure, the best results were obtained with unsubstituted (**4**, **5**, **7**–**11**) or 5-hydroxy derivatives (**22**), whereas compounds **15**, **16**, and **21** derived from 5-methoxyindole showed lower values.

In vitro BBB permeation assay

To evaluate the brain penetration of tacrine–melatonin hybrids, we used a parallel artificial membrane permeation assay for blood–brain barrier (PAMPA-BBB) by partially following the method described by Di et al.,[31] which we successfully applied to different compounds.[32] The in vitro permeabilities (P_e) of tacrine–melatonin hybrids **3**–**25** and 20 commercial drugs through a lipid extract of porcine brain were determined, and the results are listed in Table 2. Assay validation was made by comparing the experimental permeability (P_{eexptl}) with the reported values (P_{epubd}) of these commercial drugs that gave a good linear correlation: $P_{eexptl} = 0.73\,P_{epubd} + 1.48$ ($r^2 = 0.95$). From this equation, and taking into account the limits previously established for BBB permeation,[31] we found that molecules with a permeability $> 4.4 \times 10^{-6}$ cm s^{-1} are able to cross the BBB.

The assay predicted the control compounds correctly and showed that almost all tacrine–melatonin derivatives could cross the BBB and reach their biological targets located in the CNS (Table 2). Only compounds **22** and **23**, derived from 5-hydroxyindole, showed a decreased capacity for brain permeation.

Molecular modeling

With the aim of obtaining useful information about the binding interactions between tacrine–melatonin hybrids and hAChE, a molecular modeling study was performed. The active site of hAChE is composed of the catalytic triad (Ser203, Glu334, and His447) at the bottom of the gorge, the anionic subsite at Trp86, the acyl pocket at Phe295 and Phe297, and the oxyanion hole at Gly120, Gly121, and Ala204. In addition to this, the PAS at the entrance of the gorge (Tyr72 and Trp286) is of particular interest, as it is believed to play a major role in Aβ plaque formation as a key step in the development of AD.[12]

Table 3. Optimized complexes between hAChE and tacrine–melatonin hybrids. Binding energy and distances [Å] to outstanding binding subsites: CAS, hydrophobic pocket (HPP), mid-gorge, and PAS.

Compd	ΔG_{bind} [kcal mol^{-1}]	CAS			HPP[c]	Mid-Gorge		PAS		
		Trp86[a]	Tyr337[a/b]	His447		Tyr124	Arg296	Tyr72[d]	Tyr124[d/e]	Trp286[d]
1	−3.68	3.57	5.60/3.71	3.61	–	–	–	–	–	–
4	−9.31	3.36	6.05/3.91	3.69	–	4.10	2.38	4.84	4.50/4.86	6.92
5	−10.48	3.56	5.97/3.87	3.54	–	–	–	3.91	4.20/3.93	5.91
8	−11.13	3.59	6.72/4.41	3.90	3.50	–	–	3.75	4.89/4.28	4.28
9	−9.82	3.37	5.85/3.88	3.74	–	3.72	2.40	4.87	4.56/4.70	5.85
10	−10.04	3.47	6.06/3.99	3.64	3.32	3.87	2.37	4.96	4.62/4.92	5.79
11	−11.46	3.47	6.14/3.95	3.66	3.40	–	–	3.39	5.92/4.53	4.72
15	−10.55	3.48	6.11/3.87	3.58	–	3.84	2.82	5.44	4.80/5.23	5.71
16	−11.07	3.51	5.86/3.83	3.61	–	–	–	4.25	8.16/6.35	5.13
21	−11.44	3.48	6.15/3.98	3.65	3.44	–	–	3.48	7.37/5.64	4.96
22	−9.68	3.63	5.88/3.74	3.59	–	3.74	2.97	4.50	4.36/4.54	6.62

[a] Distance between the aromatic centroids of both tacrine and the corresponding amino acid. [b] Distance between the aromatic centroid of tacrine and the carbonyl oxygen atom of the amino acid. [c] Distance between the chlorine atom and the hydrophobic pocket (HPP). [d] Distance between the aromatic centroids of both indole and the corresponding aromatic amino acid. [e] Distance between the aromatic centroid of indole and the carboxylic oxygen atom of the amino acid.

Although the three-dimensional structure of hAChE is known, its complex with tacrine, the common framework to all these hybrids, has not been solved. As an alternative, we used the well-known complex between AChE from *Torpedo californica* (*Tc*AChE) and tacrine as a starting model (PDB code 1ACJ). First, the crystallographic coordinates of tacrine found in the *Tc*AChE–tacrine complex were transferred to hAChE, and then the complex was energy-minimized (see Experimental Section for details). In this optimized complex, tacrine showed only interactions with the CAS binding site of hAChE, whereas no interactions were observed with the PAS subsite (Table 3). As previously observed in the *Tc*AChE–tacrine complex,[33] the protonated nitrogen atom of the quinoline ring establishes a hydrogen bond with the carbonyl group of the main chain of His447 of the hAChE catalytic triad. In addition, the quinoline ring is π-stacked between the aromatic rings of Trp86 and Tyr337 in a sandwich arrangement. Previous structural studies showed that the Tyr337 residue (Phe330 in 1ACJ) adopts an open, closed, or half-open conformation according to angles χ_1 and χ_2, and depending on the nature of the ligand.[34] The *Tc*AChE–donepezil complex (PDB code 1EVE) is characterized by the open-gate conformation, whereas the complex with tacrine (1ACJ) displays a closed conformation, and the half-open conformation is observed in the complex between *Tc*AChE and (−)-huperzine A (1VOT).[35] In the current study, the Tyr337 residue displays a closed conformation ($\chi_1 = 166.3^\circ$ and $\chi_2 = 35.3^\circ$), as is the case for the *Tc*AChE–tacrine complex.

Similarly, we constructed models for the complexes between hAChE and tacrine–melatonin hybrids, using the same orientation for the tetrahydroquinoline ring as found in the energy-minimized hAChE–tacrine complex. The binding energy (ΔG_{bind}) of the optimized complexes gave evidence for strong interactions between the enzyme and the synthetic tacrine–melatonin hybrids. According to our rational design, these compounds occupy the entire enzymatic gorge, with strong interactions with the CAS, mid-gorge, and PAS (Table 3).

In all complexes the tacrine moiety was bound to CAS (see Table 3 and Figure 2), displaying a parallel π–π stacking interaction between Trp86 and Tyr337 [distances between aromatic centroids: 3.36–3.63 Å (Trp86) and 5.86–6.72 Å (Tyr337)]. In addition, a hydrogen bond was observed between the protonated nitrogen atom of the quinoline ring and the carbonyl group of the main chain of His447 (N···O distances: 3.54–3.90 Å). According to the average values of angles χ_1 and χ_2 (160° and 50°, respectively), the residue of Tyr337 shows a closed orientation in all cases that improved the aromatic interaction between this amino acid and the tacrine fragment.

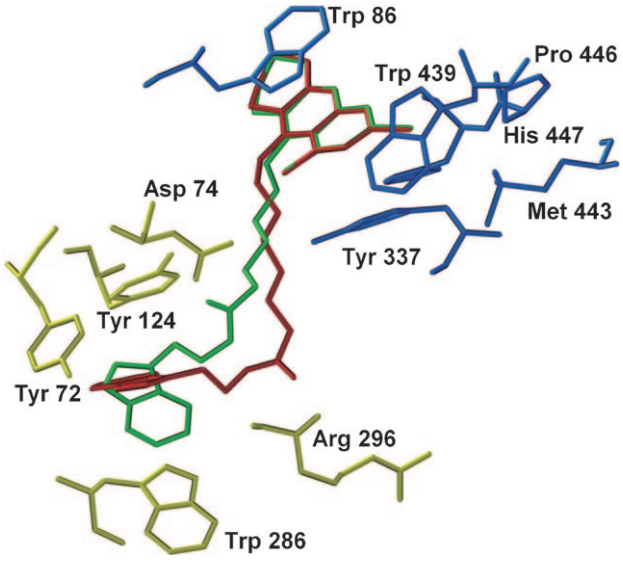

Figure 2. Hybrids **10** ($n = 5$, green) and **11** ($n = 6$, red) docked into the catalytic gorge of hAChE, highlighting the protein residues belonging to CAS (blue) and PAS (yellow) that establish the main interactions.

Regarding the 6-chloro (compound **8**) and 6,8-dichlorotacrine (**10** and **11**) derivatives, the chlorine atom at position 6

occupies a small hydrophobic pocket composed of Trp439, Met443, and Pro446, as illustrated in Figure 3. This additional interaction could explain the greater potencies of hybrids with a chlorine atom at position 6 in the tacrine ring relative to the unsubstituted counterparts.

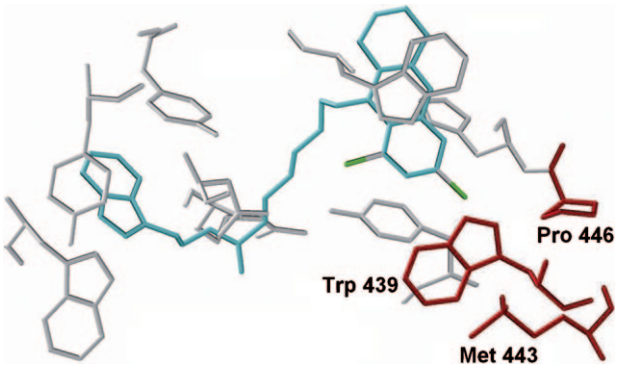

Figure 3. Interactions of hybrid **11** (cyan) with the hydrophobic pocket composed by Trp439, Met443, and Pro446 (red).

Table 4. Dihedral angles for Tyr72 and Trp286 observed in the optimized complexes.[a]

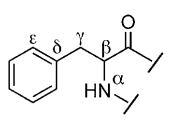

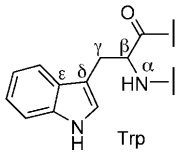

	Tyr72		Trp286	
Ligand	χ_1	χ_2	χ_1	χ_2
none	157.10	78.30	−57.57	95.16
4	212.00	107.90	168.30	90.70
5	191.10	98.60	221.30	110.20
8	200.20	98.00	232.40	102.80
9	209.10	105.90	169.70	91.10
10	189.20	93.30	172.10	86.60
11	192.20	93.20	194.80	71.20
15	189.40	95.00	161.30	98.60
16	187.80	76.90	201.60	85.00
21	193.00	85.90	207.10	73.80
22	212.50	108.40	167.70	88.70

[a] Dihedral angle χ_1: α–β–γ–δ; dihedral angle χ_2: β–γ–δ–ε.

In all tacrine–melatonin hybrids the linker is aligned along the gorge of the enzyme, where the amide group establishes the most relevant interactions. In hybrids containing five methylene units between the amine and the amide groups (compounds **4**, **9**, **10**, **15**, and **22**), the nitrogen atom belonging to the amide was hydrogen-bonded to the carbonyl oxygen of Arg296 (average N···O distance: 2.59 Å), whereas the amide oxygen was bonded to the hydroxy group of Tyr124 (average O···O distance <4.0 Å). These stabilizing interactions were not observed in hybrids with a tether of six methylene units due to the opposite orientation of the amide group (Table 3). Moreover, the 5-hydroxyindole derivative **22** showed an additional hydrogen bond between its phenolic hydroxy group and the carbonyl oxygen of Arg296 (O···O distance: 3.0 Å).

The tacrine–melatonin hybrids adopted an appropriate orientation in the PAS that allows aromatic interactions between the indole ring and the aromatic side chain of both Tyr72 and Trp286 (Table 3). Compounds containing a tether of six methylene units (**5**, **8**, **11**, **16**, and **21**) showed shorter distances to PAS residues, indicating improved π–π stacking interactions. For instance, hybrid **11** ($n=6$) showed better stabilizing interactions with PAS residues than its counterpart **10** ($n=5$, Table 3). This general feature could explain the greater hAChE inhibition of hybrids with a tether of six methylene units relative to compounds bearing linkers of five methylene units.

Finally, Tyr72 and Trp286 changed their initial orientation in the free enzyme to improve the aromatic interactions with the melatonin fragment in the final complexes, as deduced from the dihedral angles listed in Table 4. In each complex, the χ_1 angle belonging to Trp286 showed the greatest variation, indicating a stronger interaction between this residue and the melatonin fragment. Notably, hybrids with a six-methylene unit tether (**5**, **8**, **11**, **16**, and **21**) provoked higher variations in χ_1 of Trp286 than compounds with shorter linkers.

To quantify the contribution of amino acids in the binding process, variations in the solvent-accessible surface area (ΔSASA) were calculated by using Structural Thermodynamic Calculations software (v 4.3). The residues with $\Delta SASA > 4$ Å^2 are listed in Table 5, along with their partial contribution to the binding energy of the complex (ΔG_{bind}). According to the above molecular modeling studies, the most important contributions were found in the residues belonging to the CAS (Trp86, Tyr337, and His447), the mid-gorge (Tyr124 and Arg296), and the PAS (Tyr72, Asp74, and Trp286). In all complexes, aromatic interactions (Tyr72, Trp86, Trp286, and Tyr337) contribute more to complex stability than hydrogen bonds (Tyr124, Arg296, and His447). In the case of compounds with five-methylene unit linkers (**4**, **9**, **10**, **15**, and **22**) the most important aromatic contributions to ΔG_{bind} are due to Trp86 and Tyr337, both from the CAS. However, for the six-methylene unit hybrids (**5**, **8**, **11**, **16**, and **21**) Trp286 from PAS establishes the most significant aromatic binding interaction, besides the two CAS residues previously mentioned which also contribute to the stability of the final complexes of this family.

hAChE and hBuChE alignment

As previously stated, tacrine–melatonin hybrids show more affinity for hAChE than for hBuChE; this selectivity is more dramatic for compounds bearing a 6-chlorotacrine group (**7** and **8**) or a 6,8-dichlorotacrine group (**10**, **11**, and **21**). To explain this behavior, a sequence alignment of the amino acid residues of both enzymes was carried out with the ClustalX program.[36] Although hAChE and hBuChE have high homology (54% identity and 81% similarity), we found differences in some CAS and PAS residues that are involved in inhibitor binding (Figure 4). The hAChE catalytic gorge is lined by fourteen aromatic residues, whereas for hBuChE, six of these positions (Tyr72, Tyr124, Trp286, Phe295, Phe297, and Tyr337) are replaced by aliphatic

Table 5. Partial contribution [in kcal mol^{-1}] to the total binding energy [ΔG_{bind}] of amino acids involved in the binding process.[a]

Residue	1	4	5	8	9	10	11	15	16	21	22
Tyr72	--	--	--	--	--	−0.1	−0.2	−0.1	−0.4	−0.3	−0.1
Asp74	--	−0.3	0.0	0.0	−0.2	−0.2	−0.2	−0.2	−0.3	−0.4	−0.2
Thr83	--	--	--	0.1	--	--	--	--	--	--	--
Trp86	−0.4	−0.4	−0.4	−0.4	−0.4	−0.4	−0.4	−0.4	−0.4	−0.4	−0.4
Gly121	−0.4	−0.3	−0.3	−0.2	−0.3	−0.3	−0.3	−0.3	−0.3	−0.3	−0.3
Tyr124[b]	--	−0.5	−0.5	−0.6	−0.5	−0.4	−0.5	−0.5	−0.4	−0.5	−0.5
Tyr133	−0.1	−0.1	−0.1	−0.1	−0.1	−0.1	−0.1	−0.1	−0.1	−0.1	−0.1
Glu202	−0.1	−0.1	−0.2	−0.2	−0.1	−0.2	−0.2	−0.2	−0.2	−0.2	−0.2
Glu285	--	0.1	--	--	0.1	--	--	0.1	--	--	--
Trp286	--	−0.1	−0.8	−0.6	−0.2	−0.2	−0.6	−0.4	−0.8	−0.8	−0.2
Phe295	--	--	−0.1	--	--	--	−0.1	--	−0.1	--	--
Arg296[b]	--	−0.2	−0.3	−0.3	−0.2	−0.2	−0.2	−0.4	--	−0.1	−0.3
Phe297	--	--	−0.1	−0.1	−0.1	−0.1	−0.1	−0.1	−0.1	−0.1	−0.1
Ser298	--	--	−0.1	−0.2	−0.1	−0.1	−0.1	−0.1	--	--	−0.1
Tyr337	−0.3	−0.5	−0.6	−0.5	−0.5	−0.5	−0.6	−0.5	−0.6	−0.6	−0.5
Phe338	--	−0.1	--	−0.1	--	−0.1	−0.1	−0.1	−0.1	−0.1	−0.1
Tyr341	--	−0.1	−0.1	−0.1	−0.1	−0.1	−0.2	−0.1	−0.2	−0.2	−0.1
His447[b]	0.2	−0.2	−0.2	−0.2	−0.2	−0.3	−0.2	−0.2	−0.2	−0.3	−0.2

[a] Only residues with ΔSASA > 4 Å^2 were considered. [b] Hydrogen bonding.

```
1B41  DAELLVTVRGGRLRGIRLKTPGGPVSAFLGIPFAEPPMGPRRFLPPEPKQPWSGVVDATT
1P0I  ---IIIATKNGKVRGMQLTVFGGTVTAFLGIPYAQPPLGRLRFKKPQSLTKWSDIWNATK
         :::::.:.*::**::*.. **.*:******:*:**:*  **  *:.   **.: :**.
1B41  FQSVCYQYVDTLYPGFEGTEMWNPNRELSEDCLYLNVWTPYPRPTSPTPVLVWIYGGGFY
1P0I  YANSCCQNIDQSFPGFHGSEMWNPNTDLSEDCLYLNVWIPAPKPKNAT-VLIWIYGGGFQ
      : . * *▲:*  :***.*△****** :********** * *:*...* **:*******▲
1B41  SGASSLDVYDGRFLVQAERTVLVSMNYRVGAFGFLALPGSREAPGNVGLLDQRLALQWVQ
1P0I  TGTSSLHVYDGKFLARVERVIVVSMNYRVGALGFLALPGNPEAPGNMGLFDQQLALQWVQ
      ▲*:***.****:**.:.**.::*********:*******. *****:**:**:*******
1B41  ENVAAFGGDPTSVTLFGESAGAASVGMHLLSPPSRGLFHRAVLQSGAPNGPWATVGMGEA
1P0I  KNIAAFGGNPKSVTLFGESAGAASVSLHLLSPGSHSLFTRAILQSGSFNAPWAVTSLYEA
      :*:*****:*.**************.:***** *:.** **:****: *.***...: **
1B41  RRRATQLAHLVGCP--NDTELVACLRTR-PAQVLVNHEWHVLPQESVFRFSFVPVVDGDF
1P0I  RNRTLNLAKLTGCSRENETEIIKCLRNKDPQEILLN-EAFVVPYGTPLSVNFGPTVDGDF
      *.*: :**:*.**.  *:**:: ***.: * ::*:* *▲.*:*  :.△▲△ * *.*****
1B41  LSDTPEALINAGDFHGLQVLVGVVKDEGSYFLVYGAPGFSKDNESLISRAEFLAGVRVGV
1P0I  LTDMPDILLELGQFKKTQILVGVNKDEGTAFLVYGAPGFSKDNNSIITRKEFQEGLKIFF
      *:* *: *:: *:*:  *:**** **** :△************:*:*:* **  *::: .
1B41  PQVSDLAAEAVVLHYTDWLHPEDPARLREALSDVVGDHNVVCPVAQLAGRLAAQGARVYA
1P0I  PGVSEFGKESILFHYTDWVQR--PENYREALGDVVGDYNFICPALEFTKKFSEWGNNAFF
      * **::. *::::*****::   * . ****.*****:*.:**. ::: :::  * ..:
1B41  YVFEHRASTLSWPLWMGVPHGYEIEFIFGIPLDPSRNYTAEEKIFAQRLMRYWANFARTG
1P0I  YYFEHRSSKLPWPEWMGVMHGYEIEFVFGLPLER-RDYTKAEEILSRSIVKRWANFAKYG
      * ****:*.*.** ****△*******:**:**:  *:**  *:*::: ::: *****: *
1B41  DPNEPPK-APQWPPYTAGAQQYVSLDLRPLEVRRGLRAQACAFWNRFLPKLLSAT
1P0I  NPQETQNQSTSWPVFKSTEQKYLTLNTESTRIMTKLRAQQCRFWTSFFPKV----
      :*:*. : :..** :.:  *:*::*: .. .:   **** * **. *:**:
```

Figure 4. Primary sequence alignment of hAChE (PDB code 1B41) and hBuChE (PDB code 1P0I) employing the ClustalX program. [* identity, : high similarity, · moderate similarity, ▲ key CAS residues, △ key PAS residues.]

amino acids (Asn68, Gln119, Ala277, Leu286, Val288, and Ala328, respectively). Because the main forces involved in the binding between tacrine–melatonin hybrids and hAChE are π–π stacking interactions, these amino acid differences could explain the observed selectivity, because in hBuChE these interactions were diminished.

The greater selectivity toward hAChE observed in the 6-chloro (**7** and **8**) and 6,8-dichloro derivatives (**10**, **11**, and **21**) could be explained by the replacement of Pro446 in hAChE by Met437 at this position in hBuChE. Such replacement removes the hydrophobic pocket that anchors the chloride atom in hAChE; at the same time, the terminal methyl group of Met437 undergoes steric clash with the 6-chlorotacrine unit (Figure 5).

Propidium displacement assay

As mentioned in the Introduction, AChE has secondary noncholinergic functions related to fibril assembly and deposition of Aβ in AD. The structural motif of the enzyme that promotes Aβ fibril formation is located at the PAS, where Trp286 appears to play an important role.[12] Support for this hypothesis is given by studies demonstrating that, while selective CAS inhibitors do not decrease Aβ aggregation, the PAS-specific ligand propidium is able to abolish fibril formation.[37]

To determine if tacrine–melatonin hybrids are able to bind the PAS of AChE, as our molecular modeling study indicated, hybrid **8** was chosen as an illustrative compound for the series. Its experimental affinity for the PAS of AChE was studied by displacement of propidium iodide, a specific AChE PAS ligand that exhibits a 10-fold fluorescence enhancement when bound to AChE.[38] Compound **8** was evaluated at 0.3, 1.0, and 3.0 μM, showing propidium displacements of 42, 34, and 35%, respectively. 1,5-Bis-(4-allyldimethylammoniumphenyl)pentan-3-one dibromide was used as a reference compound at 3 mM, exhibiting a propidium displacement of 21%, worse than **8** at the lowest concentration tested (42% at 0.3 μM). These results confirmed the observations made in the molecular modeling study, indicating that tacrine–melatonin hybrids are able to bind to the PAS of AChE, and

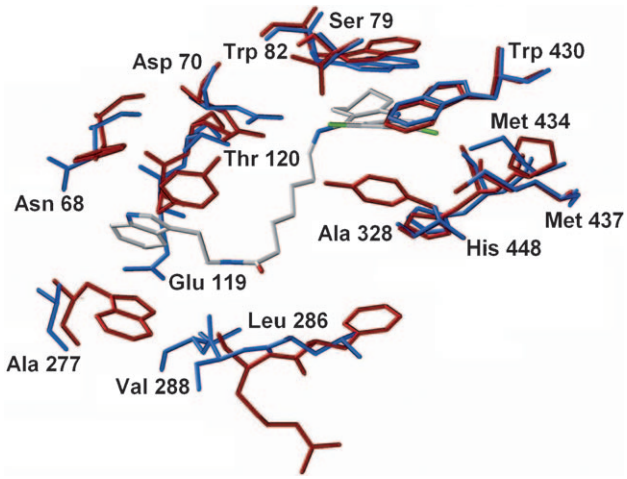

Figure 5. Superposition of complexes formed between hybrid **11** and hAChE (PDB code 1B41, red) and hBuChE (PDB code 1P0I, blue). The inhibitor is represented in gray, and the chlorine atoms are shown in green. Only the amino acid residues of hBuChE are labeled.

can therefore inhibit Aβ fibril formation promoted by this enzyme.

Effects on Aβ self-aggregation

To study the effect of tacrine–melatonin hybrids on Aβ peptide self-aggregation, a thioflavin T fluorescence assay was used. This method measures the percentage of β-sheet amyloid fibril structures of a solution of $A\beta_{1-40}$, alone or in the presence of tested compounds, using propidium as reference.[39] Hybrids **5** (tacrine–indole), **7** (6-chlorotacrine–indole), **10** (6,8-dichlorotacrine–indole), and **16** (tacrine–5-methoxyindole), showing similar inhibitory potency toward hAChE (IC_{50} = 0.5–0.7 nM) and covering the most relevant structural features in both aromatic fragments, were selected for this experiment. With the exception of **10**, these tacrine–melatonin hybrids efficiently inhibit Aβ aggregation in a range varying from 47 to 63% (Table 6), and are at least as potent as propidium, which caused 46% inhibition. The most potent hybrid is **7**, containing 6-chlorotacrine and an unsubstituted indole ring.

Cell viability and neuroprotection studies

To explore the therapeutic potential of tacrine–melatonin hybrids, cell viability and neuroprotective capacity against different toxic insults (Aβ and oxidative stress) were assayed with the human neuroblastoma cell line SH-SY5Y and the above selected hybrids **5**, **7**, **10**, and **16**. Cytotoxic effects were studied by exposing cells to compounds at two different concentrations (1 and 10 μM) for 24 h. Cell viability reached 100% when hybrids were tested at 1 μM, and was >80% when **5**, **7**, and **16** were evaluated at 10 μM (Table 6). Only hybrid **10** showed a little less cell viability (78%) when it was tested at 10 μM, probably due to the presence of two chlorine atoms in the tacrine fragment. These results indicate that tacrine–melatonin hybrids exhibit a wide therapeutic safety range.

The neuroprotective effects of compounds **5**, **7**, and **16** against the toxic action of the $A\beta_{25-35}$ fragment were determined by using a concentration range from 0.1 nM to 10 μM. As shown in Table 6, compounds showed moderate neuroprotective effects; hybrid **7** (6-chlorotacrine–indole) was the most active, with a neuroprotection percentage of 16.2±0.2% at 1 μM.

Conditions of oxidative stress in neuroblastoma cells were simulated by using hydrogen peroxide or rotenone as toxic agents. Hydrogen peroxide is a nonselective reactive species that causes lipid peroxidation and DNA damage in cells,[40] whereas rotenone is a specific inhibitor of the mitochondrial complex I and induces apoptosis by enhancing the generation of mitochondrial ROS.[41] In both experiments, the endogenous antioxidant enzyme catalase was employed as a reference (Table 6). Whereas compound **5** exerted moderate neuroprotection against the effects of hydrogen peroxide, hybrid **7** (6-chlorotacrine–indole) was able to protect cells against rotenone-induced toxicity; this neuroprotection is equal to that derived from the endogenous antioxidant enzyme catalase.

Conclusions

In summary, we have developed new tacrine–melatonin hybrids that display several interesting in vitro activities for the treatment of AD: cholinergic, antioxidant, and neuroprotective properties. They are potent and selective inhibitors of hAChE,

Table 6. Inhibition of $A\beta_{1-40}$ peptide aggregation, cell viability, and neuroprotection (NP) against both $A\beta_{25-35}$ peptide and oxidative stress by selected tacrine–melatonin hybrids at the concentrations indicated.[a]

Compd	Inhibition of $A\beta_{1-40}$ Aggregation[b]	Cell Viability[c]		NP vs. $A\beta_{25-35}$[d]				NP vs. oxidative stress[d]	
		1 μM	10 μM	0.1 nM	10 nM	1 μM	10 μM	0.3 μM	3 μM
5	47±7	100	85	3.4±0.03	5.7±0.07	9.0±0.03	2.6±0.02	19±1[e]	ND
7	63±5	100	88	4.1±0.08	10.9±0.2	16.2±0.2	9.4±0.09	ND	30±3[f]
10	≈0	100	78	ND	ND	ND	ND	ND	ND
16	47±7	100	95	0	3.4±0.06	5.7±0.06	2.3±0.05	ND	ND

[a] Results are the mean ±SEM (n = 3); ND: not determined. [b] Percentage of non-aggregated $A\beta_{1-40}$ after 24 h incubation using $A\beta_{1-40}$ at 10 μM and tested compounds (including propidium) at 100 μM; inhibition of $A\beta_{1-40}$ aggregation by propidium: 46%. [c] Percentage of cell survival after incubation with tested compounds for 24 h. [d] Percentage of cell survival after incubation with the toxic insult and the tested compound for 24 h. [e] H_2O_2 (60 μM); neuroprotection of catalase at 0.3 μM: 95%. [f] Rotenone (30 μM); neuroprotection of catalase at 3 μM: 30%.

with IC_{50} values in the nanomolar and picomolar ranges (5×10^{-9}–8×10^{-12} M), and are therefore 70- to 43000-fold more potent than tacrine. 6-Chloro- and 6,8-dichlorotacrine–melatonin derivatives show remarkable selectivity, being 200–1000-fold more active toward hAChE than hBuChE. They showed greater antioxidant properties than trolox, the aromatic portion of vitamin E responsible for radical capture, as well as melatonin itself.

In accordance with the dual interaction with both the CAS and PAS of hAChE, as shown by molecular modeling studies, these tacrine–melatonin hybrids are able to displace propidium from the PAS, and thus may be able to diminish Aβ aggregation promoted by AChE. Moreover, they inhibit Aβ self-aggregation and are at least as potent as propidium. In human neuroblastoma cells they show protective properties against damage caused by Aβ and by mitochondrial free radicals. Finally, they have low toxicity and would be able to penetrate the CNS to reach their cerebral targets.

It is therefore expected that these multifunctional products would increase patient cognition, diminish the oxidative damage caused by mitochondrial free radicals, and delay the degenerative process related to the excessive deposition of Aβ. Such outstanding properties highlight these tacrine–melatonin hybrids as very interesting multifunctional prototypes in the search for new disease-modifying agents for Alzheimer's disease.

Experimental Section

Chemistry

General procedures: Reagents and solvents were purchased from common commercial suppliers and were used without further purification. Chromatographic separations were performed on silica gel using flash-column chromatography (Kieselgel 60, Merck, 230–400 mesh), and compounds were detected with UV light ($\lambda=254$ nm). NMR spectra were recorded with a Varian XL-300 spectrometer. Typical spectral parameters for ^{1}H NMR were: spectral width 10 ppm, pulse width 9 μs (57°), data size 32 K. The acquisition parameters in decoupled ^{13}C NMR spectra were: spectral width 16 kHz, acquisition time 0.99 s, pulse width 9 μs (57°), data size 32 K. Chemical shifts (δ) are reported in ppm relative to internal Me_4Si, and J values are reported in Hz. IR spectra were recorded with a PerkinElmer Spectrum One FTIR spectrometer. HPLC analyses were performed on Waters 6000 equipment with a UV detector (λ: 214–274 nm) using a Delta Pak C_{18} 5 μm, 300 Å column. Compounds were eluted at a flow rate of 1.0 mL min^{-1}, using mixtures of CH_3CN (solvent A) and H_2O with 0.05% trifluoroacetic acid (solvent B) as indicated in each case. Melting points were determined in a Reichert–Jung Thermovar apparatus. Mass spectra were obtained by electrospray ionization (ESI) in positive mode using a Hewlett–Packard MSD 1100 spectrometer. Elemental analyses were carried out in a PerkinElmer 240C instrument. Intermediates **26**–**30** were synthesized by following published methods.[25]

General procedure for the synthesis of acids 31–35. A mixture of the appropriate 9-chloro-1,2,3,4-tetrahydroacridine **26**–**30** (1.0 mmol) and α,ω-amino acid (1.0 mmol) in pentanol (20 mL) was held a reflux overnight. After cooling to room temperature, the mixture was diluted with CH_2Cl_2 (50 mL), washed with NaOH(aq) (10%, 3×30 mL), and H_2O (3×30 mL). The organic phase was dried over Na_2SO_4 and evaporated to dryness under reduced pressure. Intermediate esters were purified by flash-column chromatography using mixtures of CH_2Cl_2/CH_3OH and then hydrolyzed with NaOH in a mixture of H_2O and dioxane (1:1). After holding at reflux for 6–18 h, the solution was cooled to room temperature and was made acidic with 2 N HCl(aq). The solvent was evaporated under reduced pressure, and the residue was purified by silica gel flash-column chromatography. Intermediates **31b,c**, **32b,c**, **33b**, **34b,c**, and **35b** were described in a previous work.[24]

5-(1,2,3,4-Tetrahydroacridin-9-ylamino)pentanoic acid (**31a**). Colorless syrup (85% yield): $R_f=0.4$ (CH_2Cl_2/CH_3OH, 8:1); ^{1}H NMR (300 MHz, CD_3OD): $\delta=8.57$ (d, $J=8.5$ Hz, 1H), 8.02 (t, $J=8.5$ Hz, 1H), 7.98 (d, $J=8.5$ Hz, 1H), 7.76 (t, $J=8.5$ Hz, 1H), 4.16 (t, $J=6.8$ Hz, 2H), 3.21 (m, 2H), 2.91 (m, 2H), 2.56 (t, $J=6.8$ Hz, 2H), 2.14 (m, 4H), 2.05 (m, 2H), 1.86 ppm (m, 2H); ^{13}C NMR (75 MHz, CD_3OD): $\delta=21.8$, 22.9, 23.0, 24.9, 29.3, 30.9, 34.1, 48.6, 112.9, 117.0, 120.1, 126.4, 126.5, 134.0, 139.7, 151.6, 157.9, 177.0 ppm; ESI-MS m/z 299 $[M+H]^+$; Anal. calcd for $C_{18}H_{22}N_2O_2$: C 72.46, H 7.43, N 9.39, found: C 72.69, H 7.76, N 8.99.

8-(1,2,3,4-Tetrahydroacridin-9-ylamino)octanoic acid (**31d**). Colorless syrup (76% yield): $R_f=0.6$ (CH_2Cl_2/CH_3OH, 13:1); ^{1}H NMR (300 MHz, CD_3OD): $\delta=8.58$ (dd, $J=8.4$ Hz, $J=1.2$ Hz, 1H), 8.04 (ddd, 1H, $J=8.4$ Hz, $J=7.1$ Hz, $J=1.2$ Hz, 1H), 7.95 (dd, $J=8.4$ Hz, $J=1.2$ Hz, 1H), 7.77 (ddd, $J=8.4$ Hz, $J=7.1$ Hz, $J=1.2$ Hz, 1H), 4.14 (t, $J=7.2$ Hz, 2H), 3.20 (t, $J=5.4$ Hz, 2H), 2.88 (t, $J=5.4$ Hz, 2H), 2.45 (t, $J=7.3$ Hz, 2H), 2.16 (m, 4H), 2.02 (quint, $J=7.3$ Hz, 2H), 1.77 (quint, $J=7.3$ Hz, 2H), 1.58 ppm (m, 6H); ^{13}C NMR (75 MHz, CD_3OD): $\delta=21.8$, 22.9, 24.8, 25.6, 27.5, 29.4, 29.8, 29.9, 31.4, 34.8, 49.1, 112.9, 117.1, 120.1, 126.3, 126.5, 134.1, 139.8, 151.7, 158.1, 177.5 ppm; ESI-MS m/z 341 $[M+H]^+$; Anal. calcd for $C_{21}H_{28}N_2O_2$: C 74.08, H 8.29, N 8.23, found: C 74.55, H 8.52, N 8.89.

8-(6,8-Dichloro-1,2,3,4-tetrahydroacridin-9-ylamino)octanoic acid (**34d**). Colorless syrup (79% yield): $R_f=0.5$ (CH_2Cl_2/CH_3OH, 15:1); ^{1}H NMR (300 MHz, CD_3OD): $\delta=7.98$ (d, $J=2.3$ Hz, 1H), 7.77 (d, $J=7.3$ Hz, 1H), 3.81 (t, $J=7.2$ Hz, 2H), 3.19 (t, $J=6.4$ Hz, 2H), 2.97 (t, $J=6.4$ Hz, 2H), 2.39 (t, $J=7.3$ Hz, 2H), 2.09 (m, 4H), 1.87 (quint, $J=7.0$ Hz, 2H), 1.72 (quint, $J=7.0$ Hz, 2H), 1.46 ppm (m, 6H); ^{13}C NMR (75 MHz, CD_3OD): $\delta=22.5$, 23.2, 25.8, 27.4, 27.7, 29.9, 30.0, 31.8, 32.5, 36.0, 50.4, 116.5, 118.8, 123.4, 128.4, 131.7, 136.0, 146.8, 155.1, 158.8, 178.9 ppm; ESI-MS m/z 409 $[M+H]^+$; Anal. calcd for $C_{21}H_{26}Cl_2N_2O_2$: C 61.62, H 6.40, N 6.84, found: C 61.99, H 6.75, N 6.43.

6-(7-Fluoro-1,2,3,4-tetrahydroacridin-9-ylamino)hexanoic acid (**35b**). Colorless syrup (80% yield): $R_f=0.6$ (CH_2Cl_2/CH_3OH, 14:1); ^{1}H NMR (300 MHz, CD_3OD): $\delta=8.25$ (dd, $^3J_{8,F}=10.7$ Hz, $J=8.5$ Hz, 1H), 8.05 (dd, $J=8.5$ Hz, $^4J_{5,F}=5.1$ Hz, 1H), 7.85 (ddd, $^3J_{6,F}=10.0$ Hz, $J=8.5$ Hz, $J=2.4$ Hz, 1H), 4.08 (t, $J=7.2$ Hz, 2H), 3.22 (m, 2H), 2.92 (m, 2H), 2.40 (t, $J=7.2$ Hz, 2H), 2.13 (m, 4H), 2.02 (quint, $J=7.2$ Hz, 2H), 1.84 (quint, $J=7.2$ Hz, 2H), 1.64 ppm (m, 2H); ^{13}C NMR (75 MHz, CD_3OD): $\delta=21.8$, 23.0, 25.3, 26.2, 27.4, 29.5, 31.3, 36.6, 48.6, 110.4 (d, $^2J_{C,F}=25.7$ Hz), 113.0, 118.1 (d, $^3J_{C,F}=9.0$ Hz), 123.1 (d, $^3J_{C,F}=9.0$ Hz), 123.3 (d, $^2J_{C,F}=26.2$ Hz), 136.7, 152.3, 157.1, 160.5 (d, $^1J_{C,F}=245.2$ Hz), 179.9 ppm; ESI-MS m/z 331 $[M+H]^+$; Anal. calcd for $C_{19}H_{23}FN_2O_2$: C 69.07, H 7.02, N 8.48, found: C 69.37, H 7.33, N 8.14.

General procedure for the synthesis of tacrine–melatonin hybrids 3–23. The appropriate 3-(2-aminoethyl)indole derivative (1.0 mmol) and then triethylamine (2.6 mmol) were added to a mixture of the corresponding acid **31**–**35** (1.0 mmol) and benzotriazol-1-yloxy)tris(dimethylamino)phosphonium hexafluorophosphate (BOP, 1.3 mmol) in CH_2Cl_2. The reaction mixture was stirred

at room temperature overnight and then diluted with CH_2Cl_2 (50 mL). The resulting mixture was consecutively washed with aqueous citric acid (10%, 3×30 mL), $NaHCO_3$(aq) (10%, 3×30 mL), and H_2O (30 mL). The organic phase was dried over Na_2SO_4 and evaporated to dryness under reduced pressure. The residue was purified on a silica gel column using mixtures of EtOAc/CH_3OH/30% NH_3(aq) as eluent, obtaining the corresponding tacrine–melatonin compound as a syrup. Subsequent treatment with HCl(g) in CH_2Cl_2 yielded the HCl salt, which was collected by filtration as a pure solid. Tacrine–melatonin hybrids **4**, **5**, **7**–**11**, **15**, **16**, **18**, **19**, **21**, and **22** were described in a previous work.[24]

***N*-(2-(1*H*-Indol-3-yl)ethyl)-5-(1,2,3,4-tetrahydroacridin-9-ylamino)-pentanamide** (**3**). Syrup (51% yield): R_f=0.3 (EtOAc/CH_3OH/30% NH_3(aq), 6:1:0.2); ^{1}H NMR (300 MHz, CD_3OD): δ=8.27 (dd, J=8.5 Hz, J=1.0 Hz, 1H), 7.95 (dd, J=8.5 Hz, J=1.0 Hz, 1H), 7.73 (ddd, J=8.5 Hz, J=6.8 Hz, J=1.0 Hz, 1H), 7.70 (dd, J=7.8 Hz, J=1.0 Hz, 1H), 7.55 (ddd, J=8.5 Hz, J=6.8 Hz, J=1.0 Hz, 1H), 7.48 (dd, J=7.8 Hz, J=1.0 Hz, 1H), 7.26 (dt, J=7.8 Hz, J=1.0 Hz, 1H), 7.22 (s, 1H), 7.15 (dt, J=7.8 Hz, J=1.0 Hz, 1H), 3.69 (t, J=6.6 Hz, 2H), 3.64 (t, J=7.2 Hz, 2H), 3.16 (m, 2H), 3.08 (t, J=7.2 Hz, 2H), 2.91 (m, 2H), 2.33 (t, J=6.6 Hz, 2H), 2.09 (m, 4H), 1.78 ppm (m, 4H); ^{13}C NMR (75 MHz, CD_3OD): δ=23.6, 24.0, 24.4, 26.7 (2C), 31.6, 33.3, 36.6, 41.3, 48.6, 112.2, 113.3, 116.7, 119.3, 119.6, 121.6, 122.2, 123.3, 124.5, 124.9, 127.5, 128.8, 129.9, 138.1, 147.9, 153.4, 158.7, 175.7 ppm; IR (KBr): $\tilde{\nu}$=3413, 3256, 2933, 2863, 1635, 1588, 1523, 1457, 1410, 1357, 1252, 747 cm^{-1}; ESI-MS *m/z* 441 $[M+H]^+$; **3**·HCl: pale-yellow solid; mp: 105–107 °C; HPLC (A/B, 80:20) t_R=8.16 min (98%); Anal. calcd for $C_{28}H_{32}N_4O$·HCl: C 70.50, H 6.97, N 11.74, found: C 70.83, H 7.25, N 11.52.

***N*-(2-(1*H*-Indol-3-yl)ethyl)-8-(1,2,3,4-tetrahydroacridin-9-ylamino)octanamide** (**6**). Syrup (65% yield): R_f=0.5 (EtOAc/CH_3OH/30% NH_3(aq), 9:1:0.2); ^{1}H NMR (300 MHz, CD_3OD): δ=8.37 (dd, J=8.5 Hz, J=1.0 Hz, 1H), 7.93 (dd, J=8.5 Hz, J=1.0 Hz, 1H), 7.82 (ddd, J=8.5 Hz, J=6.8 Hz, J=1.0 Hz, 1H), 7.71 (dd, J=7.7 Hz, J=1.0 Hz, 1H), 7.61 (ddd, J=8.5 Hz, J=6.8 Hz, J=1.0 Hz, 1H), 7.49 (dd, J=7.7 Hz, J=1.0 Hz, 1H), 7.23 (dt, J=7.7 Hz, J=1.0 Hz, 1H), 7.21 (s, 1H), 7.15 (dt, J=7.7 Hz, J=1.0 Hz, 1H), 3.84 (t, J=7.3 Hz, 2H), 3.65 (t, J=7.3 Hz, 2H), 3.15 (m, 2H), 3.10 (t, J=7.3 Hz, 2H), 2.91 (m, 2H), 2.31 (t, J=7.3 Hz, 2H), 2.09 (m, 4H), 1.86 (quint, J=7.3 Hz, 2H), 1.72 (quint, J=7.3 Hz, 2H), 1.54 ppm (m, 6H); ^{13}C NMR (75 MHz, CD_3OD): δ=23.0, 23.7, 25.6, 26.3, 26.6, 27.5, 28.0, 30.4, 31.9, 32.2, 36.9, 41.3, 48.4, 112.7, 113.7, 115.0, 119.4, 119.7, 120.0, 122.7, 123.8, 124.1, 125.2, 126.0, 129.3, 132.6, 138.6, 143.9, 155.4, 156.2, 176.6 ppm; IR (KBr): $\tilde{\nu}$=3419, 3262, 2931, 2852, 1636, 1590, 1524, 1460, 1358, 1298, 1161, 986, 844, 747, 557 cm^{-1}; ESI-MS *m/z* 483 $[M+H]^+$; **6**·HCl: pale-yellow solid; mp: 85–87 °C; HPLC (A/B, 80:20) t_R=9.95 min (99%); Anal. calcd for $C_{31}H_{38}N_4O$·HCl: C 71.72, H 7.57, N 10.79, found: C 71.43, H 7.27, N 10.41.

***N*-(2-(1*H*-Indol-3-yl)ethyl)-8-(6,8-dichloro-1,2,3,4-tetrahydroacridin-9-ylamino)octanamide** (**12**). Syrup (29% yield): R_f=0.6 (EtOAc/CH_3OH/30% NH_3(aq), 12:1:0.2); ^{1}H NMR (300 MHz, CD_3OD): δ=7.84 (d, J=2.2 Hz, 1H), 7.71 (dd, J=7.8 Hz, J=1.0 Hz, 1H), 7.62 (d, J=2.2 Hz, 1H), 7.47 (dd, J=7.8 Hz, J=1.0 Hz, 1H), 7.23 (dt, J=7.8 Hz, J=1.0 Hz, 1H), 7.21 (s, 1H), 7.13 (dt, J=7.8 Hz, J=1.0 Hz, 1H), 3.62 (t, J=7.3 Hz, 2H), 3.52 (t, J=7.3 Hz, 2H), 3.13 (t, J=6.5 Hz, 2H), 3.08 (t, J=7.3 Hz, 2H), 2.92 (t, J=6.5 Hz, 2H), 2.30 (t, J=7.3 Hz, 2H), 2.05 (m, 4H), 1.74 (m, 4H), 1.45 ppm (m, 6H); ^{13}C NMR (75 MHz, CD_3OD): δ=23.9, 24.4, 26.7, 27.4, 27.9, 28.3, 30.4 (2C), 32.5, 34.7, 37.6, 41.8, 51.0, 112.7, 113.7, 118.3, 119.7, 120.0, 121.2, 122.7, 123.8, 127.4, 128.6, 129.3, 131.1, 135.5, 138.6, 150.2, 154.7, 159.4, 176.4 ppm; IR (KBr): $\tilde{\nu}$=3402, 3272, 2930, 2855, 1737, 1643, 1594, 1575, 1543, 1457, 1434, 1339, 1114, 988, 951, 848, 791, 741 cm^{-1}; ESI-MS *m/z* 551 $[M+H]^+$; **12**·HCl: pale-yellow solid; mp: 95–96 °C; HPLC (A/B, 80:20) t_R=8.48 min (98%); Anal. calcd for $C_{31}H_{36}Cl_2N_4O$·HCl: C 63.32, H 6.34, N 9.53, found: C 63.53, H 6.71, N 9.89.

***N*-(2-(1*H*-Indol-3-yl)ethyl)-6-(7-fluoro-1,2,3,4-tetrahydroacridin-9-ylamino)hexanamide** (**13**). Syrup (50% yield): R_f=0.7 (EtOAc/CH_3OH/30% NH_3(aq), 6:1:0.2); ^{1}H NMR (300 MHz, CD_3OD): δ=8.17 (dd, $^3J_{H,F}$=10.6 Hz, J=2.5 Hz, 1H), 7.90 (dd, J=8.2 Hz, $^4J_{H,F}$=5.0 Hz, 1H), 7.82 (ddd, $^3J_{H,F}$=10.6 Hz, J=8.2 Hz, J=2.5 Hz, 1H), 7.63 (dd, J=7.8 Hz, J=1.0 Hz, 1H), 7.43 (dd, J=7.8 Hz, J=1.0 Hz, 1H), 7.18 (s, 1H), 7.16 (dt, J=7.8 Hz, J=1.0 Hz, 1H), 7.08 (dt, J=7.8 Hz, J=1.0 Hz, 1H), 3.98 (t, J=7.3 Hz, 2H), 3.60 (t, J=7.3 Hz, 2H), 3.07 (m, 2H), 3.02 (t, J=7.3 Hz, 2H), 2.80 (m, 2H), 2.36 (t, J=7.3 Hz, 2H), 2.05 (m, 4H), 1.94 (quint, J=7.3 Hz, 2H), 1.80 (quint, J=7.3 Hz, 2H), 1.59 ppm (m, 2H); ^{13}C NMR (75 MHz, CD_3OD): δ=26.1, 21.6, 22.8, 24.9, 26.3, 26.9, 29.2, 31.0, 36.8, 41.3, 48.5, 110.5 (d, $^2J_{C,F}$=25.7 Hz), 112.1 (2C), 113.0 (d, $^3J_{C,F}$=7.0 Hz), 117.9, 119.2, 119.5, 122.2, 122.7 (d, $^3J_{C,F}$=9.0 Hz), 123.4, 123.6 (d, $^2J_{C,F}$=26.2 Hz), 128.7, 136.3, 137.9, 151.9, 157.2, 160.4 (d, $^1J_{C,F}$=245.3 Hz), 175.9 ppm; IR (KBr): $\tilde{\nu}$=3430, 2939, 2863, 1638, 1598, 1528, 1458, 1253, 1220, 1099, 836, 742, 559 cm^{-1}; ESI-MS *m/z* 473 $[M+H]^+$; **13**·HCl: pale-yellow solid; mp: 90–92 °C; HPLC (A/B, 80:20) t_R=6.36 min (100%); Anal. calcd for $C_{29}H_{33}FN_4O$·HCl: C 68.42, H 6.73, N 11.01, found: C 68.78, H 6.95, N 11.34.

***N*-[2-(5-Methoxy-1*H*-indol-3-yl)ethyl]-5-(1,2,3,4-tetrahydroacridin-9-ylamino)pentanamide** (**14**). Syrup (33% yield): R_f=0.4 (EtOAc/CH_3OH/30% NH_3(aq), 6:1:0.2); ^{1}H NMR (300 MHz, CD_3OD): δ=8.35 (dd, J=8.5 Hz, J=1.2 Hz, 1H), 7.92 (dd, J=8.5 Hz, J=1.2 Hz, 1H), 7.84 (ddd, J=8.5 Hz, J=6.6 Hz, J=1.2 Hz, 1H), 7.65 (ddd, J=8.5 Hz, J=6.6 Hz, J=1.2 Hz, 1H), 7.34 (d, J=8.8 Hz, 1H), 7.20 (d, J=2.5 Hz, 1H), 7.19 (s, 1H), 6,87 (dd, J=8.8 Hz, J=2.5 Hz, 1H), 3.97 (s, 3H), 3.80 (t, J=7.3 Hz, 2H), 3.63 (t, J=7.2 Hz, 2H), 3.14 (m, 2H), 3.04 (t, J=7.3 Hz, 2H), 2.87 (m, 2H), 2.37 (t, J=7.3 Hz, 2H), 2.10 (m, 4H), 1.73 ppm (m, 4H); ^{13}C NMR (75 MHz, CD_3OD): δ=23.4, 24.1, 24.4, 26.1, 26.8, 31.8, 32.7, 37.4, 41.7, 48.2, 56.7, 101.8, 112.9, 113.3, 113.5, 115.8, 120.1, 124.7, 125.2, 125.7, 125.8, 129.6, 131.9, 138.8, 145.1, 155.4, 155.6, 156.6, 176.2 ppm; IR (KBr): $\tilde{\nu}$=3414, 2934, 1643, 1590, 1523, 1486, 1453, 1358, 1298, 1200, 1174, 1128, 1070, 1035, 985, 845, 799, 753, 718, 556 cm^{-1}; ESI-MS *m/z* 471 $[M+H]^+$; **14**·HCl: pale-yellow solid; mp: 84–86 °C; HPLC (A/B, 80:20) t_R=6.50 min (99%); Anal. calcd for $C_{29}H_{34}N_4O_2$·HCl: C 68.69, H 6.96, N 11.05, found: C 68.97, H 6.67, N 11.37.

***N*-[2-(5-Methoxy-1*H*-indol-3-yl)ethyl]-8-(1,2,3,4-tetrahydroacridin-9-ylamino)octanamide** (**17**). Syrup (29% yield): R_f=0.4 (EtOAc/CH_3OH/30% NH_3(aq), 7:1:0.2); ^{1}H NMR (300 MHz, CD_3OD): δ=8.25 (dd, J=8.5 Hz, J=1.0 Hz, 1H), 7.94 (dd, J=8.5 Hz, J=1.0 Hz, 1H), 7.72 (ddd, J=8.5 Hz, J=6.6 Hz, J=1.0 Hz, 1H), 7.53 (ddd, J=8.5 Hz, J=6.6 Hz, J=1.0 Hz, 1H), 7.36 (d, J=8.8 Hz, 1H), 7.22 (d, J=2.5 Hz, 1H), 7.20 (s, 1H), 6.91 (dd, J=8.8 Hz, J=2.5 Hz, 1H), 3.98 (s, 3H), 3.77 (t, J=7.3 Hz, 2H), 3.63 (t, J=7.3 Hz, 2H), 3.16 (m, 2H), 3.08 (t, J=7.3 Hz, 2H), 2.92 (m, 2H), 2.31 (t, J=7.2 Hz, 2H), 2.10 (m, 4H), 1.78 (m, 4H), 1.50 ppm (m, 6H); ^{13}C NMR (75 MHz, CD_3OD): δ=23.8, 24.3, 26.4, 26.8, 27.3, 28.2, 30.5 (2C), 32.6, 33.8, 37.4, 41.7, 49.2, 56.8, 101.8, 113.2, 113.4, 113.5, 116.6, 121.1, 124.7, 125.3, 125.5, 127.0, 129.6, 131.0, 133.8, 146.9, 154.6, 155.4, 158.2, 176.7 ppm; IR (KBr): $\tilde{\nu}$=3265, 2930, 2855, 1645, 1579, 1522, 1487, 1456, 1357, 1296, 1213, 1173, 1072, 1036, 984, 924, 830, 797, 756, 679, 639, 558 cm^{-1}; ESI-MS *m/z* 513 $[M+H]^+$; **17**·HCl: pale-yellow solid; mp: 55–57 °C; HPLC (A/B, 80:20) t_R=10.48 min (99%); Anal. calcd for $C_{32}H_{40}N_4O_2$·HCl: C 71.72, H 7.57, N 10.79, found: C 71.92, H 7.87, N 10.43.

6-(6,8-Dichloro-1,2,3,4-tetrahydroacridin-9-ylamino)-*N*-(2-(5-methoxy-1*H*-indol-3-yl)ethyl)hexanamide (**20**). Syrup (68% yield): R_f = 0.7 (EtOAc/CH_3OH/30% NH_3(aq), 9:1:0.2); ^{1}H NMR (300 MHz, CD_3OD): δ 7.80 (d, J = 2.2 Hz, 1H), 7.63 (d, J = 2.2 Hz, 1H), 7.34 (d, J = 8.7 Hz, 1H), 7.21 (s, 1H), 7.20 (d, J = 2.4 Hz, 1H), 6.86 (dd, J = 8.7 Hz, J = 2.4 Hz, 1H), 3.97 (s, 3H), 3.62 (t, J = 7.2 Hz, 2H), 3.56 (t, J = 7.2 Hz, 2H), 3.12 (t, J = 6.3 Hz, 2H), 3.04 (t, J = 7.2 Hz, 2H), 2.92 (t, J = 6.3 Hz, 2H), 2.30 (t, J = 7.2 Hz, 2H), 2.04 (m, 4H), 1.79 (quint, J = 7.0 Hz, 2H), 1.72 (quint, J = 7.0 Hz, 2H), 1.44 ppm (m, 2H); ^{13}C NMR (75 MHz, CD_3OD): δ = 22.8, 23.6, 26.3, 26.5, 27.2, 27.3, 31.6, 32.5, 36.9, 41.2, 50.5, 56.3, 101.3, 112.4, 112.8, 113.0, 116.6, 118.9, 124.2, 124.3, 128.4, 129.1, 131.2, 133.3, 135.5, 147.2, 154.8, 155.6, 159.0, 175.9 ppm; IR (KBr): $\tilde{\nu}$ = 3410, 2936, 2863, 1627, 1577, 1535, 1486, 1458, 1351, 1216, 1174, 846, 558 cm^{-1}; ESI-MS m/z 553 $[M+H]^+$; **20**·HCl: pale-yellow solid; mp: 83–85 °C; HPLC (A/B, 80:20) t_R = 5.23 min (98%); Anal. calcd for $C_{30}H_{34}Cl_2N_4O_2$·HCl: C 61.07, H 5.98, N 9.50, found: C 61.37, H 6.25, N 9.83.

***N*-[2-(5-Hydroxy-1*H*-indol-3-yl)ethyl]-8-(1,2,3,4-tetrahydroacridin-9-ylamino)octanamide** (**23**). Syrup (39% yield): R_f = 0.5 (EtOAc/CH_3OH/30% NH_3(aq), 7:1:0.2); ^{1}H NMR (300 MHz, CD_3OD): δ = 8.28 (dd, J = 8.5 Hz, J = 1.2 Hz, 1H), 7.93 (dd, J = 8.5 Hz, J = 1.2 Hz, 1H), 7.74 (ddd, J = 8.5 Hz, J = 6.6 Hz, J = 1.2 Hz, 1H), 7.55 (ddd, J = 8.5 Hz, J = 6.6 Hz, J = 1.2 Hz, 1H), 7.32 (d, J = 8.5 Hz, 1H), 7.16 (s, 1H), 7.10 (d, J = 2.4 Hz, 1H), 6.83 (dd, J = 8.5 Hz, J = 2.4 Hz, 1H), 3.71 (t, J = 7.1 Hz, 2H), 3.61 (t, J = 7.3 Hz, 2H), 3.13 (m, 2H), 3.02 (t, J = 7.3 Hz, 2H), 2.88 (m, 2H), 2.29 (t, J = 7.1 Hz, 2H), 2.06 (m, 4H), 1.80 (quint, J = 7.2 Hz, 2H), 1.71 (quint, J = 7.2 Hz, 2H), 1.48 ppm (m, 6H); ^{13}C NMR (75 MHz, CD_3OD): δ = 41.2, 23.4, 23.9, 25.9, 26.3, 26.8, 27.6, 30.0 (2C), 32.1, 33.5, 37.0, 49.6, 103.5, 112.3, 112.5, 112.6, 116.2, 120.7, 124.4, 124.7, 124.9, 126.8, 129.5, 130.3, 133.0, 146.8, 151.1, 153.9, 158.0, 176.1 ppm; IR (KBr): $\tilde{\nu}$ = 3255, 2998, 2889, 2849, 2807, 1644, 1590, 1527, 1460, 1299, 1200, 1068, 986, 844, 749 cm^{-1}; ESI-MS m/z 499 $[M+H]^+$; **23**·HCl: pale-yellow solid; mp: 108–110 °C; HPLC (A/B, 80:20) t_R = 4.63 min (100%); Anal. calcd for $C_{31}H_{38}N_4O_2$·HCl: C 69.58, H 7.35, N 10.47, found: C 69.79, H 7.68, N 10.78.

General procedure for the synthesis of thioamides 24 and 25. Lawesson's reagent (LR, 1.5 mmol) was added to a solution of **4** or **6** (1.0 mmol) in toluene (anhyd, 10 mL), and the mixture was held a reflux for 8 h. It was then cooled to room temperature and purified by silica gel flash-column chromatography. Subsequent treatment with HCl(g) in CH_2Cl_2 yielded the HCl derivative as a pure solid that was collected by filtration.

***N*-(2-(1*H*-Indol-3-yl)ethyl)-6-(1,2,3,4-tetrahydroacridin-9-ylamino)-hexanethioamide** (**24**). Syrup (60% yield): R_f = 0.7 (EtAcO/CH_3OH/30% NH_3(aq), 8:1:0.2); ^{1}H NMR (300 MHz, CD_3OD): δ = 8.55 (dd, J = 8.0 Hz, J = 1.0 Hz, 1H), 7.93 (dd, J = 8.0 Hz, J = 1.0 Hz, 1H), 7.78 (dd, J = 8.0 Hz, J = 1.0 Hz, 1H), 7.76 (ddd, J = 8.0 Hz, J = 6.3 Hz, J = 1.0 Hz, 1H), 7.58 (ddd, J = 8.0 Hz, J = 6.3 Hz, J = 1.0 Hz, 1H), 7.48 (dd, J = 8.0 Hz, J = 1.0 Hz, 1H), 7.23 (dt, J = 8.0 Hz, J = 1.0 Hz, 1H), 7.21 (s, 1H), 7.15 (dt, J = 8.0 Hz, J = 1.0 Hz, 1H), 4.11 (t, J = 7.3 Hz, 2H), 4.02 (t, J = 7.2 Hz, 2H), 3.22 (t, J = 7.2 Hz, 2H), 3.10 (m, 2H), 2.91 (m, 2H), 2.76 (t, J = 7.2 Hz, 2H), 2.09 (m, 4H), 1.86 (quint, J = 7.1 Hz, 2H), 1.80 (quint, J = 7.1 Hz, 2H), 1.58 ppm (m, 2H); ^{13}C NMR (75 MHz, CD_3OD): δ = 21.8, 22.9, 24.4, 26.2, 29.2, 29.5, 31.0, 36.9, 46.3, 47.9, 49.6, 112.2, 113.0, 116.2, 119.5, 119.6, 120.0, 122.3, 123.4, 124.8, 125.0, 126.3, 128.8, 130.4, 138.2, 147.3, 154.0, 157.9, 206.3 ppm; IR (KBr): $\tilde{\nu}$ = 3240, 3040, 2932, 2875, 1633, 1587, 1522, 1455, 1355, 1252, 1102, 751, 677, 620 cm^{-1}; ESI-MS m/z 471 $[M+H]^+$; **24**·HCl: yellow solid; mp: 121–123 °C; HPLC (A/B, 80:20) t_R = 7.6 min (99%); Anal. calcd for $C_{29}H_{34}N_4S$·HCl: C 68.68, H 6.96, N 11.05, found: C 68.98, H 7.25, N 11.37.

***N*-(2-(1*H*-Indol-3-yl)ethyl)-8-(1,2,3,4-tetrahydroacridin-9-ylamino)octanethioamide** (**25**). Syrup (87% yield): R_f = 0.7 (EtOAc/CH_3OH/30% NH_3(aq), 9:1:0.2); ^{1}H NMR (300 MHz, CD_3OD): δ = 8.32 (dd, J = 8.0, J = 1.0 Hz, 1H), 7.93 (dd, J = 8.0 Hz, J = 1.0 Hz, 1H), 7.78 (dd, J = 7.0 Hz, J = 1.1 Hz, 1H), 7.76 (ddd, J = 8.0 Hz, J = 6.3 Hz, J = 1.0 Hz, 1H), 7.58 (ddd, J = 8.0 Hz, J = 6.3 Hz, J = 1.0 Hz, 1H), 7.48 (dd, J = 7.9 Hz, J = 1.1 Hz, 1H), 7.23 (dt, J = 7.9 Hz, J = 1.1 Hz, 1H), 7.21 (s, 1H), 7.15 (dt, J = 7.9 Hz, J = 1.1 Hz, 1H), 4.06 (t, J = 7.3 Hz, 2H), 3.76 (t, J = 7.3 Hz, 2H), 3.25 (t, J = 7.3 Hz, 2H), 3.15 (m, 2H), 2.91 (m, 2H), 2.72 (t, J = 7.3 Hz, 2H), 2.09 (m, 4H), 1.84 (m, 4H), 1.50 ppm (m, 6H); ^{13}C NMR (75 MHz, CD_3OD): δ = 23.4, 23.9, 24.4, 25.9, 27.6, 29.5, 29.9, 30.4, 32.1, 33.4, 46.9, 47.5, 49.6, 112.2, 113.0, 116.2, 119.5, 119.6, 120.6, 122.3, 123.4, 124.8, 125.0, 126.7, 128.8, 130.4, 138.2, 147.3, 154.0, 157.9, 206.1 ppm; IR (KBr): $\tilde{\nu}$ = 3245, 3049, 2930, 2855, 1635, 1589, 1522, 1458, 1357, 1261, 1102, 802, 751, 679, 618 cm^{-1}; ESI-MS m/z 499 $[M+H]^+$; **25**·HCl: yellow solid; mp: 113–115 °C; HPLC (A/B, 80:20) t_R = 6.9 min (100%); Anal. calcd for $C_{31}H_{38}N_4S$·HCl: C 69.57, H 7.35, N 10.47, found: C 69.87, H 7.68, N 10.85.

Molecular modeling methods

The simulation system was based on the X-ray crystallographic structure of tacrine (**1**) in complex with AChE from *Torpedo californica* (*Tc*AChE; PDB code 1ACJ), owing to its high degree of identity with hAChE (PDB code 1B41). The coordinates of **1** from the pattern complex *Tc*AChE–**1** were transferred to the hAChE structure, and this new complex, hAChE–**1**, was used as a model to study the binding mode of the tacrine–melatonin hybrids with the human enzyme. All calculations were performed on a Silicon Graphics Octane workstation (300 MHz MIPS R12000 (IP30) processor), using the Sketch Molecule of SYBYL 6.9 to construct the molecules. In all cases, the MMFF94 force field was applied with the use of distant-dependent dielectric constants and a conjugate gradient method until the gradient reached 0.05 kcal mol^{-1} Å^{-1}. The molecules were manually positioned within the binding pocket of the enzyme, taking into account the experimental data about well-known inhibitors. The manual minimization of complexes maintained a rigid enzyme backbone, using the MMFF94 force field until the gradient reached 0.05 kcal mol^{-1} Å^{-1}. These complexes were the input structures for docking using the FlexiDock command within SYBYL 6.9. During the flexible docking analysis, the protein was considered rigid except the residues involved in the binding site, and the ligands were considered flexible. Conformers were classified in different families taking into account: 1) the binding energy from the FlexiDock results, 2) the main interactions between the inhibitor and the binding sites of the enzyme (CAS, PAS, and mid-gorge) using the Ligand Protein Contact (LPC) program,[42] and 3) the Gibbs energy of binding (ΔG_{bind}) calculated with Structural Thermodynamic Calculations (STC) software v 4.3.[43] The representative molecules from all groups were re-optimized using the above mentioned conditions.

Biochemical methods

In vitro cholinesterase inhibition assay. AChE from bovine erythrocytes (0.25–1.0 U mg^{-1}, lyophilized powder), AChE from human erythrocytes (minimal 500 U (mg protein)$^{-1}$ in buffered aqueous solution), BuChE from equine serum (10 U (mg protein)$^{-1}$, lyophilized powder), and BuChE from human serum (3 U (mg protein)$^{-1}$, lyophilized powder) were purchased from Sigma. Compounds were evaluated in 100 mM phosphate buffer (pH 8.0) at 30 °C, using acetylthiocholine and butyrylthiocholine (0.4 mM) as sub-

strates, respectively. In both cases, 5,5′-dithiobis(2-nitrobenzoic)acid (DTNB, Ellman's reagent, 0.2 mM) was used, and IC_{50} values were calculated by UV/Vis spectroscopy from the absorbance changes at $\lambda = 412$ nm.[26] Experiments were performed in triplicate.

Oxygen radical absorbance capacity assay. The ORAC-FL method of Ou et al.[29a] partially modified by Dávalos et al.[29b] was followed, using a Polarstar Galaxy plate reader (BMG Labtechnologies GmbH, Offenburg, Germany) with 485-P excitation and 520-P emission filters. The equipment was controlled by the Fluostar Galaxy software (v 4.11-0) for fluorescence measurement. 2,2′-Azobis(amidinopropane) dihydrochloride (AAPH), (±)-6-hydroxy-2,5,7,8-tetramethylchromane-2-carboxylic acid (trolox), and fluorescein (FL) were purchased from Sigma–Aldrich. The reaction was carried out in 75 mM phosphate buffer (pH 7.4), and the final reaction mixture was 200 μM. Antioxidant (20 μL) and fluorescein (120 μL; 70 nM final concentration) solutions were placed in a black 96-well microplate (96F untreated, Nunc™). The mixture was pre-incubated for 15 min at 37 °C, and the AAPH solution (60 μL; 12 mM final concentration) was then added rapidly with a multichannel pipette. The microplate was immediately placed in the reader, and the fluorescence was recorded every minute for 80 min. The microplate was automatically shaken prior to each reading. Samples were measured at eight different concentrations (0.1–1 μM). A blank (FL + AAPH) using phosphate buffer instead of the sample solution and eight calibration solutions using trolox (1–8 μM) were also carried out in each assay. All reaction mixtures were prepared in duplicate, and at least three independent assays were performed for each sample. Antioxidant curves (fluorescence versus time) were first normalized to the curve of the blank corresponding to the same assay, and then the area under the fluorescence decay curve (AUC) was calculated. The net AUC corresponding to a sample was calculated by subtracting the AUC corresponding to the blank. Regression equations between net AUC and antioxidant concentration were calculated for all the samples. ORAC-FL values were expressed as trolox equivalents by using the standard curve calculated for each assay. Final results were expressed as (μmol trolox equivalent)/(μmol pure compound).

In vitro BBB permeation assay. Prediction of brain penetration was evaluated using a parallel artificial membrane permeation assay (PAMPA) in a similar manner as described previously.[31,32] Commercial drugs, phosphate-buffered saline (PBS, pH 7.4), and dodecane were purchased from Sigma–Aldrich, Acros, and Fluka. Millex filter units (PVDF membrane, ∅ = 25 mm, pore size 0.45 μm) were acquired from Millipore. The porcine brain lipid (PBL) was obtained from Avanti Polar Lipids. The donor microplate was a 96-well filter plate (PVDF membrane, pore size 0.45 μm), and the acceptor microplate was an indented 96-well plate, both from Millipore. The acceptor 96-well microplate was filled with 170 μL PBS/EtOH (9:1), and the filter surface of the donor microplate was impregnated with 4 μL porcine brain lipid (PBL) in dodecane (20 mg mL^{-1}). Compounds were dissolved in PBS/EtOH (9:1) at 1 mg mL^{-1}, filtered through a Millex filter, and then added to the donor wells (170 μL). The donor filter plate was carefully put on the acceptor plate to form a sandwich, which was left undisturbed for 120 min at 25 °C. After incubation, the donor plate was carefully removed, and the concentration of compounds in the acceptor wells was determined by UV/Vis spectroscopy. Every sample was analyzed at five wavelengths, in four wells, and in at least three independent runs, and the results are given as the mean ± SD. In each experiment, 20 quality control standards of known BBB permeability were included to validate the analysis set.

Measurement of propidium iodide displacement from the peripheral anionic site (PAS) of AChE. A solution of AChE from bovine erythrocytes at a concentration of 5 μM in 0.1 mM Tris buffer (pH 8.0) was used. Aliquots of compounds were added to give final concentrations of 0.3, 1.0, and 3.0 μM, and the solutions were kept at room temperature for at least 6 h. Afterward, the samples were incubated for 15 min with propidium iodide at a final concentration of 20 μM, and the fluorescence ($\lambda_{ex} = 485$ nm, $\lambda_{em} = 620$ nm) was measured in a fluorescence microplate reader (Fluostar Optima, BMG, Germany).

Inhibition of β-amyloid peptide aggregation: thioflavin T-based fluorimetric assay. The thioflavin T fluorescence method was used.[39] $A\beta_{1-40}$ peptide lyophilized from HFIP solution (rPeptide, Bogart, GA, USA) was dissolved in DMSO to obtain a 2.3 mM solution. Aliquots of Aβ in DMSO were then incubated with constant rotation for 24 h at room temperature in 0.215 M sodium phosphate buffer (pH 8.0) at a final Aβ concentration of 10 μM in the presence or absence of compounds or propidium at 100 μM, used as reference. Analyses were performed with a Fluostar Optima plate reader (BMG). Fluorescence was measured at 450 nm (λ_{ex}) and 485 nm (λ_{em}). To determine fibril formation after incubation, solutions containing Aβ or Aβ plus AChE inhibitors were added to 50 mM glycine-NaOH buffer (pH 8.5) containing 3 μM thioflavin T in a final volume of 150 μL. Each assay was run in triplicate and measured at various time points (0–24 h). The fluorescence intensities were recorded, and the percent aggregation was calculated by the following expression: $100-(I_{Fi}/I_{F0}\times 100)$ in which I_{Fi} and I_{F0} are the fluorescence intensities obtained for Aβ in the presence and absence of inhibitor, respectively, after subtracting the fluorescence of respective blanks.[44]

Culture of SH-SY5Y cells and studies of cell viability and neuroprotection. SH-SY5Y cells, at passages between 3 and 16 after thawing, were maintained in Dulbecco's modified Eagle's medium (DMEM) containing 15 nonessential amino acids and supplemented with 10% fetal calf serum, 1 mM glutamine, 50 U mL^{-1} penicillin, and 50 μg mL^{-1} streptomycin (reagents from GIBCO, Madrid, Spain). Cultures were seeded into flasks containing supplemented medium and were maintained at 37 °C in 5% CO_2/humidified air. Stock cultures were passaged 1:4 twice weekly. For assays, SH-SY5Y cells were sub-cultured in 48-well plates at a seeding density of 10^5 cells per well. For the cytotoxicity experiments, cells were treated with drugs before confluence, in serum-free DMEM.

To study the cytotoxic effects of the compounds alone, cells were plated at a density of 10^5 cells per well at least 48 h before toxicity measurements. Cells were exposed for 24 h to the compound at various concentrations, and the quantitative assessment of cell death was made by measurement of the percentage of the intracellular enzyme lactate dehydrogenase (LDH) released to the extracellular medium (cytotoxicity detection kit, Roche). The quantity of LDH was evaluated in a microplate reader (Anthos 2010 or Labsystems iMES Reader MS) at 492 nm (λ_{ex}) and 620 nm (λ_{em}). Controls were taken as having 100% viability. To study the cytoprotective action of various compounds against cell death induced by 200 μM $A\beta_{25-35}$, 60 μM H_2O_2, or 30 μM rotenone, drugs were given at t_0 and maintained for 24 h. The media were then replaced by fresh media still containing the drug plus cytotoxic stimulus, and cells were left for an additional 24 h period. Cell survival was assessed measuring LDH activity.

Measurement of lactic dehydrogenase (LDH) activity. Extracellular and intracellular LDH activity was measured by UV/Vis using a cytotoxicity cell death kit (Roche–Boehringer, Mannheim, Germany)

according to the manufacturer's protocol. Total LDH activity was defined as the sum of intracellular and extracellular LDH activity, and released LDH was defined as the percentage of extracellular versus total LDH activity. Data were expressed as the mean ± SEM of at least three different cultures in quadruplicate. LDH released was calculated for each individual experiment, considering as 100% the extracellular LDH released by the vehicle with respect to the total. To determine percent protection, LDH release was normalized as follows: in each individual triplicate experiment, LDH release obtained in untreated cells (basal) was subtracted from the LDH released upon the toxic treatment and normalized to 100%, and that value was subtracted from 100.

Acknowledgements

The authors gratefully acknowledge financial support from the Spanish Ministry of Science and Innovation (SAF 2006–01249 and SAF 2006–08540), Comunidad de Madrid (Programa de Actividades de I+D entre Grupos de Investigación en Biociencias, S-SAL/0275/2006), and the Spanish Ministry of Health (Instituto de Salud Carlos III, RETICS-RD06/0026). The predoctoral fellowships to M.I.F.-B. and G.C.G.-M. from CSIC (I3P Program) are also acknowledged. We also thank Mr. V. Gálvez for technical assistance. The Sociedad Española de Química Terapéutica awarded the "Laboratorios Almirall Prize for Young Researchers—2005" to a part of this work.

Keywords: Alzheimer's disease · cholinergic · drug design · molecular modeling · neuroprotection

[1] *Topics in Medicinal Chemistry: Alzheimer's Disease, Vol. 2*, (Eds: L.-F. Lau, M. A. Brodney), Springer, Berlin, **2008**, pp. 1–24.
[2] a) U. Holzgrabe, P. Kapková, V. Alptüzün, J. Scheiber, E. Kugelmann, *Expert Opin. Ther. Targets* **2007**, *11*, 161–179; b) R. M. Lane, S. G. Potkin, A. Enz, *Int. J. Neuropsychopharmacol.* **2006**, *9*, 101–124.
[3] a) P. M. Doraiswamy, *CNS Drugs* **2002**, *16*, 811–824; b) A. Castro, S. Conde, M. I. Rodríguez-Franco, A. Martínez, *Mini-Rev. Med. Chem.* **2002**, *2*, 37–50.
[4] a) G. Brousseau, B. P. Rourke, B. Burke, *Exp. Clin. Psychopharmacol.* **2007**, *15*, 546–554; b) M. Villarroya, A. G. García, J. Marco-Contelles, M. G. López, *Expert Opin. Invest. Drugs* **2007**, *16*, 1987–1998.
[5] C. G. Parsons, A. Stöffler, W. Danysz, *Neuropharmacology* **2007**, *53*, 699–723.
[6] Source: Alzheimer Research Forum, Alzforum, http://www.alzforum.org/ (accessed February 27, 2009).
[7] a) R. Bullock, A. Dengiz, *Int. J. Clin. Pract.* **2005**, *59*, 817–822; b) E. Giacobini, *J. Neural Transm. Suppl.* **2002**, 181–187.
[8] a) P. J. Modrego, *Curr. Med. Chem.* **2006**, *13*, 3417–3424; b) K. R. Krishnan, H. C. Charles, P. M. Doraiswamy, J. Mintzer, R. Weisler, X. Yu, C. Perdomo, J. R. Ieni, S. Rogers, *Am. J. Psychiatry* **2003**, *160*, 2003–2011.
[9] a) Y. Takada-Takatori, T. Kume, Y. Ohgi, Y. Izumi, T. Niidome, T. Fujii, H. Sugimoto, A. Akaike, *J. Neurosci. Res.* **2008**, *86*, 3575–3583; b) Y. W. Liu, C. Y. Li, J. L. Luo, W. M. Li, H. J. Fu, Y. Z. Lao, L. J. Liu, Y. P. Pang, D. C. Chang, Z. W. Li, R. W. Peoples, Y. X. Ai, Y. F. Han, *Biochem. Biophys. Res. Commun.* **2008**, *369*, 1007–1011; c) P. M. Kemp, C. Holmes, S. Hoffmann, S. Wilkinson, M. Zivanovic, J. Thom, L. Bolt, J. Fleming, D. G. Wilkinson, *J. Neurol. Neurosurg. Psychiatry* **2003**, *74*, 1567–1570.
[10] a) A. Musiał, M. Bajda, B. Malawska, *Curr. Med. Chem.* **2007**, *14*, 2654–2679; b) M. Racchi, E. Porrello, C. Lanni, S. C. Lenzken, M. Mazzucchelli, S. Govoni, *Aging Clin. Exp. Res.* **2006**, *18*, 149–152.
[11] A. E. Reyes, M. A. Chacón, M. C. Dinamarca, W. Cerpa, C. Morgan, N. C. Inestrosa, *Am. J. Pathol.* **2004**, *164*, 2163–2174.
[12] a) G. V. de Ferrari, M. A. Canales, I. Shin, L. M. Weiner, I. Silman, N. C. Inestrosa, *Biochemistry* **2001**, *40*, 10447–10457; b) G. Johnson, S. Moore, *Biochem. Biophys. Res. Commun.* **1999**, *258*, 758–762.
[13] a) A. Castro, A. Martínez, *Curr. Pharm. Des.* **2006**, *12*, 4377–4387; b) A. Castro, A. Martínez, *Mini-Rev. Med. Chem.* **2001**, *1*, 267–272.
[14] a) M. del Monte-Millán, E. García-Palomero, R. Valenzuela, P. Usán, C. de Austria, P. Muñoz-Ruiz, L. Rubio, I. Dorronsoro, A. Martínez, M. Medina, *J. Mol. Neurosci.* **2006**, *30*, 85–88; b) A. Castro, P. Muñoz, A. Martínez in *Medicinal Chemistry of Alzheimer's Disease* (Ed.: A. Martinez), Transworld Research Network, Kerala, **2008**, pp. 21–44; c) E. García-Palomero, P. Muñoz, P. Usán, P. García, E. Delgado, C. de Austria, R. Valenzuela, L. Rubio, M. Medina, A. Martínez, *Neurodegener. Dis.* **2008**, *5*, 153–156.
[15] A. Nunomura, R. J. Castellani, X. Zhu, P. I. Moreira, G. Perry, M. A. Smith, *J. Neuropathol. Exp. Neurol.* **2006**, *65*, 631–641.
[16] a) F. Gu, M. Zhu, J. Shi, Y. Hu, Z. Zhao, *Neurosci. Lett.* **2008**, *440*, 44–48; b) P. I. Moreira, M. S. Santos, C. R. Oliveira, J. C. Shenk, A. Nunomura, M. A. Smith, X. Zhu, G. Perry, *CNS Neurol. Disord. Drug Targets* **2008**, *7*, 3–10; c) C. Goldsbury, I. T. Whiteman, E. V. Jeong, Y.-A. Lim, *Aging Cell* **2008**, *7*, 771–775.
[17] a) A. Nunomura, G. Perry, M. A. Smith in *Oxidative Stress and Neurodegenerative Disorders* (Eds.: G. A. Qureshi, S. H. Parvez), Elsevier, Amsterdam, **2007**, pp. 451–466; b) H. Y. Zhang, D. P. Yang, G. Y. Tang, *Drug Discovery Today* **2006**, *11*, 749–754.
[18] For recently described tacrine-based ChE inhibitors, see for example: a) L. Fang, D. Appenroth, M. Decker, M. Kiehntopf, C. Roegler, T. Deufel, C. Fleck, S. Peng, Y. Zhang, J. Lehmanyn, *J. Med. Chem.* **2008**, *51*, 713–716; b) P. W. Elsinghorst, J. S. Cieslik, K. Mohr, C. Tränkle, M. Gütschow, *J. Med. Chem.* **2007**, *50*, 5685–5695; c) D. Muñoz-Torrero, P. Camps, *Curr. Med. Chem.* **2006**, *13*, 399–422; d) J. Marco-Contelles, R. León, C. de Los Ríos, A. Guglietta, J. Terencio, M. G. López, A. G. García, M. Villarroya, *J. Med. Chem.* **2006**, *49*, 7607–7610; e) P. Muñoz-Ruiz, L. Rubio, E. García-Palomero, I. Dorronsoro, M. Monte-Millán, R. Valenzuela, P. Usán, C. Austria, M. Bartolini, V. Andrisano, A. Bidon-Chanal, M. Orozco, F. J. Luque, M. Medina, A. Martínez, *J. Med. Chem.* **2005**, *48*, 7223–7233.
[19] a) R. J. Reiter, D.-X. Tan, L. C. Manchester, M. P. Terron, L. J. Flores, S. Koppisepi, *Adv. Med. Sci.* **2007**, *52*, 11–28; b) S. R. Pandi-Perumal, V. Srinivasan, G. J. M. Maestroni, D. P. Cardinali, B. Poeggeler, R. Hardeland, *FEBS J.* **2006**, *273*, 2813–2838.
[20] a) J. G. Masilamoni, E. P. Jesudason, S. Dhandayuthapani, B. S. Ashok, S. Vignesh, W. C. Jebaraj, S. F. Paul, R. Jayakumar, *Free Radical Res.* **2008**, *42*, 661–673; b) D. Acuña-Castroviejo, G. Escames, M. I. Rodríguez, L. C. López, *Front. Biosci.* **2007**, *12*, 947–963; c) C. Tomás-Zapico, A. Coto-Montes, *J. Pineal Res.* **2005**, *39*, 99–104.
[21] a) M. I. Rodríguez-Franco, M. I. Fernández-Bachiller, C. Pérez, A. Castro, A. Martínez, *Bioorg. Med. Chem.* **2005**, *13*, 6795–6802; b) M. I. Rodríguez-Franco, I. Dorronsoro, A. Castro, A. Martínez, A. Badía, J. E. Baños, *Bioorg. Med. Chem.* **2003**, *11*, 2263–2268; c) M. I. Rodríguez-Franco, I. Dorronsoro, C. Pérez, A. Castro, A. Martínez, *Med. Chem. Res.* **2002**, *12*, 333–344; d) M. I. Rodríguez-Franco, I. Dorronsoro, A. Badía, J. E. Baños, *Arch. Pharm.* **2002**, *335*, 339–346; e) M. I. Rodríguez-Franco, M. I. Fernández-Bachiller, *Synthesis* **2002**, 911–915; f) M. I. Rodríguez-Franco, M. I. Fernández-Bachiller, *Magn. Reson. Chem.* **2002**, *40*, 549–550; g) M. I. Rodríguez-Franco, I. Dorronsoro, A. I. Hernández-Higueras, G. Antequera, *Tetrahedron Lett.* **2001**, *42*, 863–865; h) M. I. Rodríguez-Franco, I. Dorronsoro, A. Martínez, *Synthesis* **2001**, 1711–1715; i) A. Martínez, E. Fernández, A. Castro, S. Conde, M. I. Rodríguez-Franco, J. E. Baños, A. Badía, *Eur. J. Med. Chem.* **2000**, *35*, 913–922; j) M. I. Rodríguez-Franco, I. Dorronsoro, A. Martínez, C. Pérez, A. Badía, J. E. Baños, *Arch. Pharm.* **2000**, *333*, 118–122.
[22] a) A. Cavalli, M. L. Bolognesi, A. Minarini, M. Rosini, V. Tumiatti, M. Recanatini, C. Melchiorre, *J. Med. Chem.* **2008**, *51*, 347–372; b) A. Cavalli, M. L. Bolognesi, S. Capsoni, V. Andrisano, M. Bartolini, E. Margotti, A. Cattaneo, M. Recanatini, C. Melchiorre, *Angew. Chem.* **2007**, *119*, 3763–3766; *Angew. Chem. Int. Ed.* **2007**, *46*, 3689–3692; c) M. Decker, *Mini-Rev. Med. Chem.* **2007**, *7*, 221–229; d) C. J. Van der Schyf, W. J. Geldenhuys, M. B. Youdim, *J. Neurochem.* **2006**, *99*, 1033–1048.
[23] a) Y. P. Pang, P. Quiram, T. Jelacic, F. Hong, S. Brimijoin, *J. Biol. Chem.* **1996**, *271*, 23646–23649; b) X. Q. Xiao, N. T. Lee, P. R. Carlier, Y. Pang, Y. F. Han, *Neurosci. Lett.* **2000**, *290*, 197–200.

[24] M. I. Rodríguez-Franco, M. I. Fernández-Bachiller, C. Pérez, B. Hernández-Ledesma, B. Bartolomé, *J. Med. Chem.* **2006**, *49*, 459–462.
[25] a) P. R. Carlier, Y. F. Han, E. S.-H. Chow, T. X. Lieu, *Bioorg. Med. Chem.* **1999**, *7*, 351–357; b) H. Ming-Kuan, M. K. Hu, L. J. Wu, M. H. Yen, *J. Med. Chem.* **2002**, *45*, 2277–2282.
[26] G. L. Ellman, K. D. Courteney, V. Andres, Jr., R. M. Teatherstone, *Biochem. Pharmacol.* **1961**, *7*, 88–95.
[27] M. Cyglerm, J. D. Scharg, J. L. Sussman, M. Harel, I. Silman, M. K. Gentry, B. P. Doctor, *Protein Sci.* **1993**, *2*, 366–382.
[28] D. R. Liston, J. A. Nielsen, A. Villalobos, D. Chapin, S. B. Jones, S. T. Hubbard, I. A. Shalaby, A. Ramirez, D. Nason, W. F. White, *Eur. J. Pharmacol.* **2004**, *486*, 9–17.
[29] a) B. Ou, M. Hampsch-Woodill, R. L. Prior, *J. Agric. Food Chem.* **2001**, *49*, 4619–4626; b) A. Dávalos, C. Gómez-Cordobés, B. Bartolomé, *J. Agric. Food Chem.* **2004**, *52*, 48–54.
[30] E. Sofic, Z. Rimpapa, Z. Kundurovic, A. Sapcanin, I. Tahirovic, A. Rustembegoric, G. Cao, *J. Neural Transm.* **2005**, *112*, 349–358.
[31] L. Di, E. H. Kerns, K. Fan, O. J. McConnell, G. T. Carter, *Eur. J. Med. Chem.* **2003**, *38*, 223–232.
[32] a) F. Reviriego, M. I. Rodríguez-Franco, P. Navarro, E. García-España, M. Liu-González, B. Verdejo, A. Domènech, *J. Am. Chem. Soc.* **2006**, *128*, 16458–16459; b) F. J. Pavón, L. Hernández-Folgado, A. Bilbao, A. Cippitelli, N. Jagerovic, G. Abellán, M. I. Rodríguez-Franco, A. Serrano, M. Macías, M. Navarro, P. Goya, F. Rodríguez de Fonseca, *Neuropharmacology* **2006**, *51*, 358–366.
[33] C. H. T. P. da Silva, V. L. Campo, I. Carvalho, C. A. Taft, *J. Mol. Graphics Modell.* **2006**, *25*, 169–175.
[34] G. Kryger, I. Silman, J. L. Sussman, *Structure* **1999**, *7*, 297–307.
[35] Q. Xie, Y. Tang, W. Li, X.-H. Wang, Z.-B. Qiu, *J. Mol. Model.* **2006**, *12*, 390–397.
[36] J. D. Tompson, T. J. Gibson, F. Plewniak, F. Jeanmougin, D. G. Higgins, *Nucleic Acids Res.* **1997**, *25*, 4876–4882.
[37] N. C. Inestrosa, A. Alvarez, C. A. Pérez, R. D. Moreno, M. Vicente, C. Linker, O. I. Casanueva, C. Soto, J. Garrido, *Neuron* **1996**, *16*, 881–891.
[38] P. Taylor, S. Lappi, *Biochemistry* **1975**, *14*, 1989–1997.
[39] a) H. LeVine III, *Protein Sci.* **1993**, *2*, 404–410; b) H. LeVine III, *Methods Enzymol.* **1999**, *309*, 274–284.
[40] B. Halliwell, O. I. Aruoma, *FEBS Lett.* **1991**, *281*, 9–19.
[41] I. Sipos, L. Tretter, V. Adam-Vizi, *J. Neurochem.* **2003**, *84*, 112–118.
[42] V. Sobolev, A. Sorokine, J. Prilusky, E. E. Abola, M. Edelman, *Bioinformatics* **1999**, *15*, 327–332.
[43] P. Lavigne, J. R. Bagu, R. Boyko, L. Willard, C. F. Holmes, B. D. Sykes, *Protein Sci.* **2000**, *9*, 252–264.
[44] M. Bartolini, C. Bertucci, V. Cavrini, V. Andrisano, *Biochem. Pharmacol.* **2003**, *65*, 407–416.

Received: December 2, 2008
Revised: February 12, 2009
Published online on ■■ ▮▮, 2009

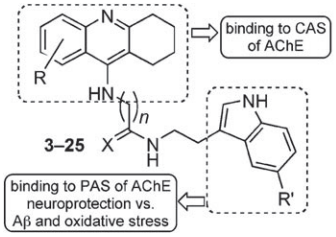

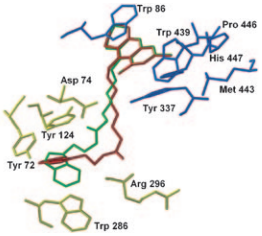

Tacrine–melatonin hybrids are potential multifunctional drugs for Alzheimer's disease that may simultaneously palliate intellectual deficits and protect the brain against both β-amyloid peptide and oxidative stress. Molecular modeling studies show that they target both the catalytic active site (CAS) and the peripheral anionic site (PAS) of AChE. They are nontoxic and may be able to penetrate the CNS, according to in vitro PAMPA-BBB assays.

*M. I. Fernández-Bachiller, C. Pérez, N. E. Campillo, J. A. Páez, G. C. González-Muñoz, P. Usán, E. García-Palomero, M. G. López, M. Villarroya, A. G. García, A. Martínez, M. I. Rodríguez-Franco**

■■ – ■■

Tacrine–Melatonin Hybrids as Multifunctional Agents for Alzheimer's Disease, with Cholinergic, Antioxidant, and Neuroprotective Properties

